Identification of macaque dendritic cell precursors in blood and tissue reveals their dysregulation in early SIV infection

Margaux Gardet, Oscar Haigh, Florian Meurisse, Sixtine Coindre, Nastasia Dimant, Delphine Desjardins, Christine Bourgeois, Bruno Vaslin, Francis Relouzat, Roger Le Grand, et al.

Cell Reports

Article

Identification of macaque dendritic cell precursors in blood and tissue reveals their dysregulation in early SIV infection

Graphical abstract

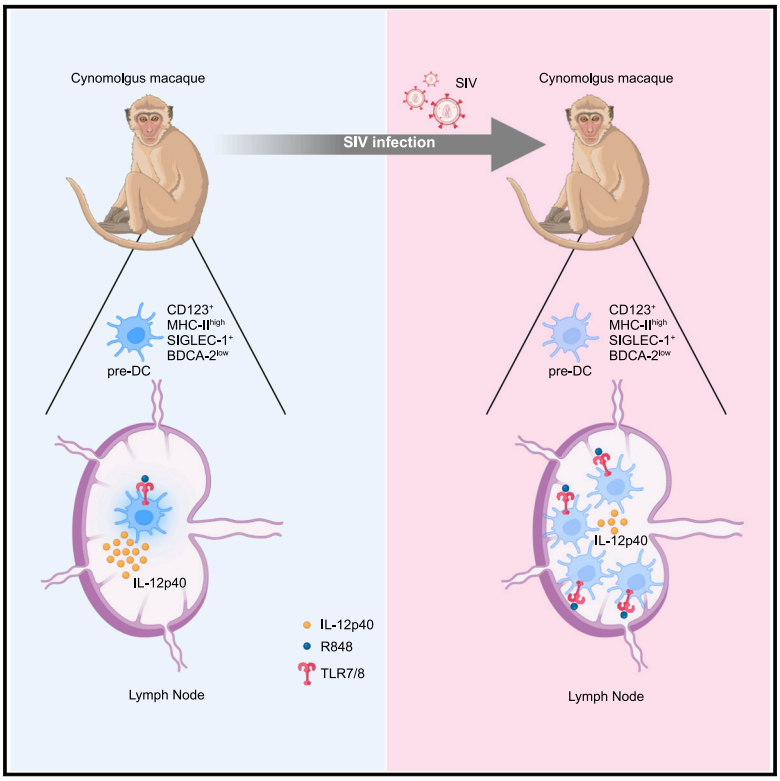

Highlights

- Identification of human pre-DC equivalent in macaques
- Pre-DCs accumulate in the lymph node from early SIV infection
- IL-12p40 production capacity of lymph node pre-DCs is attenuated in SIV infection
- T cell activation in HIV controllers correlates with pre-DC costimulatory markers

Authors

Margaux Gardet, Oscar Haigh, Florian Meurisse, ..., Roger Le Grand, Olivier Lambotte, Benoit Favier

Correspondence

benoit.favier@cea.fr

In brief

Gardet et al. define the human equivalent of dendritic cell precursors (pre-DCs) in a monkey model of HIV infection to demonstrate their accumulation in lymph nodes but without activating properly. This insight provides a better understanding of how HIV interferes with the immune response in humans.

Gardet et al., 2024, Cell Reports *43*, 113994
April 23, 2024
https://doi.org/10.1016/j.celrep.2024.113994

CellPress

Cell Reports

CellPress
OPEN ACCESS

Article

Identification of macaque dendritic cell precursors in blood and tissue reveals their dysregulation in early SIV infection

Margaux Gardet,[1] Oscar Haigh,[1,4] Florian Meurisse,[1,4] Sixtine Coindre,[1] Nastasia Dimant,[1] Delphine Desjardins,[1] Christine Bourgeois,[1] Cecile Goujard,[2,3] Bruno Vaslin,[1] Francis Relouzat,[1] Roger Le Grand,[1] Olivier Lambotte,[1,2] and Benoit Favier[1,5,*]

[1]Université Paris-Saclay, Inserm, CEA, Center for Immunology of Viral, Auto-immune, Hematological and Bacterial Diseases (IMVA-HB/IDMIT), 92265 Fontenay-aux-Roses, France

[2]Paris-Saclay University Hospital Group, Assistance Publique Hôpitaux de Paris, Department of Internal Medicine and Clinical Immunology, Bicêtre Hospital, le Kremlin-Bicêtre, France

[3]Centre de Recherche en Épidémiologie et Santé des Populations (CESP), INSERM U1018, University Paris Saclay, Paris, France

[4]These authors contributed equally

[5]Lead contact

*Correspondence: benoit.favier@cea.fr

https://doi.org/10.1016/j.celrep.2024.113994

SUMMARY

Distinct dendritic cell (DC) subsets play important roles in shaping immune responses. Circulating DC precursors (pre-DCs) are more susceptible to HIV infection *in vitro*, which may explain the inefficiency of immune responses against HIV. However, the interplay between HIV and pre-DC is not defined *in vivo*. We identify human pre-DC equivalents in the cynomolgus macaque and then analyze their dynamics during simian immunodeficiency virus (SIV) infection to illustrate a sharp decrease of blood pre-DCs in early SIV infection and accumulation in lymph nodes (LNs), where they neglect to upregulate CD83/CD86 or MHC-II. Additionally, SIV infection attenuates the capacity of stimulated LN pre-DCs to produce IL-12p40. Analysis of HIV cohorts provides correlation between costimulatory molecule expression on pre-DCs and T cell activation in spontaneous HIV controllers. These findings pinpoint certain dynamics and functional changes of pre-DCs during SIV infection, providing a deeper understanding of immune dysregulation mechanisms elicited in people living with HIV.

INTRODUCTION

Dendritic cells (DCs) are heterogeneous, including conventional (cDC1 and 2) and plasmacytoid (pDC) subsets, which play critical roles in the orchestration of immune responses thanks to their unique capacity to sense pathogens and produce immune-regulatory signals.[1–3] cDC1 and cDC2 elicit T cell responses by presenting foreign antigens alongside costimulatory molecules and further fine-tune immune outcomes through the production of cytokines. pDCs also express major histocompatibility complex (MHC)-II and synthesize cytokines but have a unique capacity to produce high amounts of type-I interferons (IFNs).[4] Following pathogen sensing, cDCs and pDCs become activated and then mature and migrate to secondary lymphoid tissues to initiate innate and adaptive immune responses. Several studies have investigated DC ontogeny and have found a unique subset of circulating dendritic cell precursors (pre-DCs) in human peripheral blood.[5–8] Produced in the bone marrow (BM), pre-DCs transit through the bloodstream into peripheral tissues and secondary lymphoid organs to seed themselves and start their differentiation process into cDC1 or cDC2. Human pre-DCs share some surface markers with pDCs, including CD123, and can produce interleukin (IL)-12 and tumor necrosis factor (TNF)-α. However, unlike pDCs, pre-DCs do not produce type-I IFNs following Toll-like receptor (TLR) stimulation.[7] Despite their precursor phenotype, human pre-DCs express high levels of MHC-II and can stimulate $CD4^+$ T cell proliferation *in vitro*.[7–9] Exceeding their precursor ability, the functional capacity of pre-DCs allows them to also contribute to initiating immune responses against pathogens.

Upon HIV infection, pDCs and cDCs can sense virus through different pattern-recognition receptors, including TLR3 and 8 for cDC1, TLR8 for cDC2, and TLR7 for pDC.[1] However, it is now well established that cDC and pDC functions are subverted by HIV-1.[10–13] cDC2 phenotype, antigen presentation, and cytokine production capacity are altered during acute HIV-1 infection.[14–17] This immune dysregulation of cDC2 persists in chronic infection and is associated with the rate of disease progression.[18–21] The role of cDC1 in HIV infection has been less investigated, but this subset is likely responsible for eliciting HIV-specific IFN-γ-producing CD8 T cells, and their decline during chronic HIV infection supports their beneficial role in anti-viral

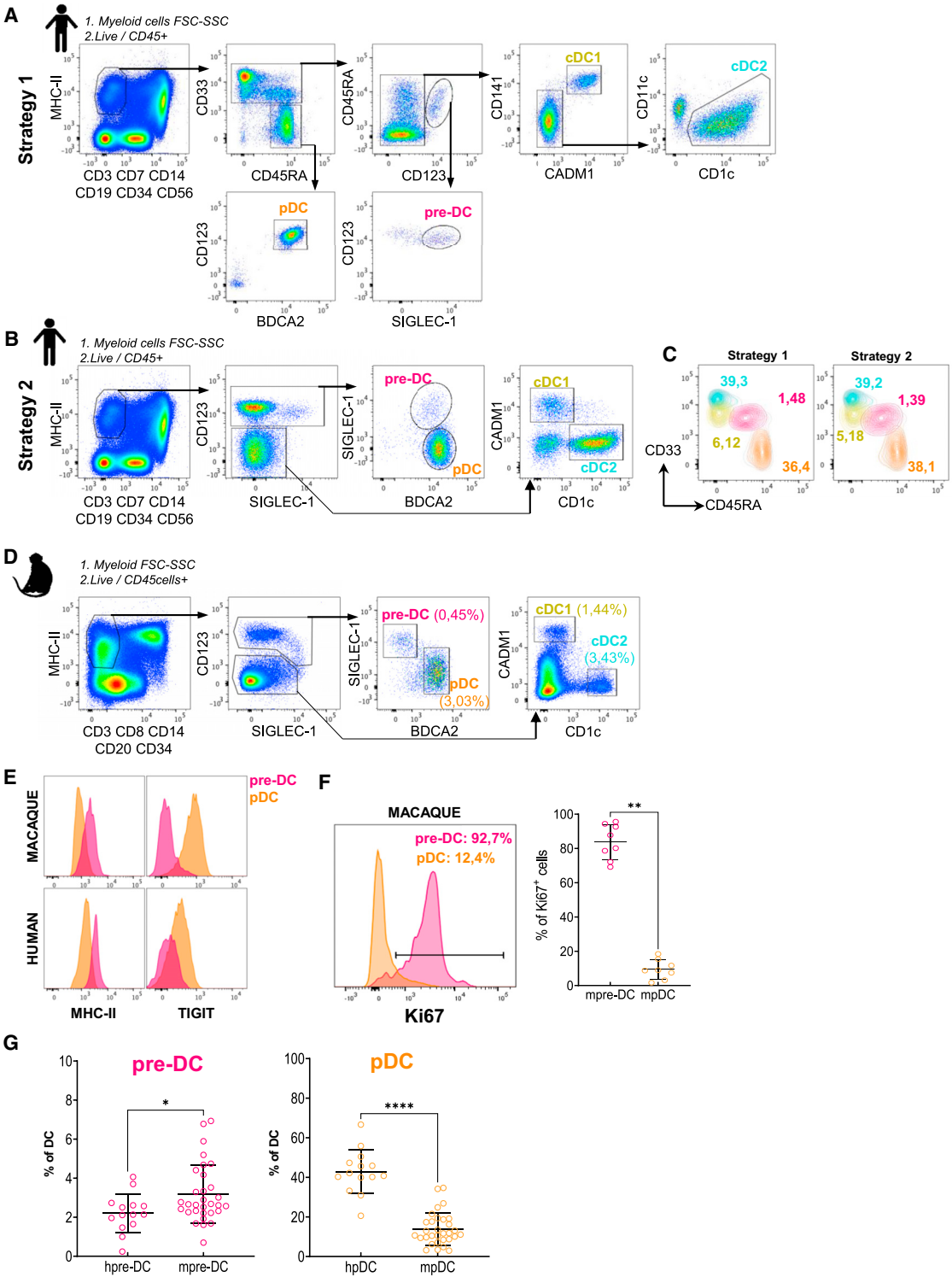

Figure 1. Identification of human pre-DC equivalent in cynomolgus macaque

(A) Representative flow cytometry strategy of the different human DC HLA-DR$^+$ subpopulations identifying CD33$^-$ CD45RA$^+$ CD123$^+$ BDCA2$^+$ pDC (orange), CD33$^+$ CD45RA^{mid} CD123$^+$ Siglec-1$^+$ pre-DC (red), CD33$^+$ CD123$^-$ CADM1$^+$ CD141$^+$ cDC1 (green), and CD33$^+$ CD123$^-$ CD141$^-$ CD1c$^+$ cDC2 (blue).

(B) Representative flow cytometry strategy of the different human DC subpopulations identifying CD123$^+$ BDCA2$^+$ Siglec-1$^-$ pDC (orange), CD123$^+$ Siglec-1$^+$ BDCA2^{mid} pre-DC (red), CD123$^-$ CADM1$^+$ cDC1 (green), and CD123$^-$ CD1c$^+$ cDC2 (blue).

(legend continued on next page)

immunity.[22,23] In early HIV infection, pDCs sense virus through TLR7 to induce a robust but transitory production of type-I IFN that dampens viral replication and initiates immune responses.[24–26] However, persistent production of type-I IFN by pDCs during chronic infection is presumed to be deleterious and favors disease progression.[25–28] cDC2s are susceptible to HIV infection, as they can be infected *in vitro*, whereas cDC1 and pDC display a resistance.[29] However, both cDC and pDC are involved in HIV dissemination, by capturing viral particles in the absence of viral replication, and then migrating to secondary lymphoid organs where they transmit virions to $CD4^+$ T cells.[30–36]

Recently, pre-DCs were identified as a major target of HIV infection *in vitro* compared to other DC subsets, and they could efficiently transfer virus to T cells.[37,38] To better understand their role in the mechanisms driving the dysregulation of immune responses and viral spreading during HIV infection, the characterization of pre-DC dynamics *in vivo* is extremely important. This is a given, considering their potential to prime and shape immune responses directly, their role in renewal of cDC1 and cDC2 pools, and their potential to disseminate infectious virions.

In this regard, macaque models of simian immunodeficiency virus (SIV) infection are the most relevant for recapitulating pathogenic HIV infection and are essential for the characterization of DC behavior within the host during HIV infection in blood and secondary lymphoid organs. This model has been instrumental, by us and others, for exploring cDC and pDC dynamics during SIV infection for HIV disease hallmarks.[39–44] Even though pre-DCs are more susceptible to HIV infection than other DC subsets *in vitro*, the effects of HIV infection on pre-DC dynamics and function remain uncharacterized *in vivo*. Furthermore, to date, pre-DCs remain undefined in macaques and during SIV infection.

We addressed this shortfall by developing a flow cytometry strategy for the characterization of human-equivalent pre-DCs in the cynomolgus macaque. We then used it to monitor their dynamics during the course of SIV infection in the blood and secondary lymphoid organs of infected animals and then assessed their phenotypic and functional response to TLR agonists. Additionally, we analyzed circulating pre-DCs from people living with HIV (PLWH), at different stages of infection. Our findings define a decrease of pre-DC during early HIV infection in PLWH, concordant with that observed in SIV-infected macaques. As well, expression of costimulatory molecules on pre-DCs positively correlated with the level of T cell activation in PLWH who spontaneously control HIV replication. Overall, this study revealed profound changes in pre-DC dynamics and dysregulation during HIV/SIV infection.

RESULTS

Multiparameter flow cytometry analysis defines human pre-DC equivalents in cynomolgus macaques

Since pre-DCs were undefined in non-human primates, a flow cytometry strategy was first designed to discriminate circulating human-equivalent pre-DCs from other equivalent DC subsets in cynomolgus macaque, as previously reported in humans[38] (Figure 1A). Our data indicate that this strategy does not work for macaque samples, since expressions of CD45RA or CD33 were not detected on pre-DCs, and no expression of CD45RA was observed on pDCs, in contrast to human subsets (Figures 1A and S1A). However, a combination of CD123, Siglec-1, and BDCA-2 staining in humans (*HLA-DR*$^+$ *CD123*$^+$ *Siglec-1*$^+$ *BDCA-2*$^+$ *lin*$^-$ cells; Figure 1B) overcame the need for CD45RA and CD33 discrimination (Figures 1A–1C). Thus, this strategy effectively discriminated pre-DCs from pDC, cDC1, and cDC2 subsets in cynomolgus macaque peripheral blood mononuclear cells (PBMCs) (Figure 1D). Applied to human PBMCs, this gating correctly identified pre-DCs as the Axl^+ $Siglec\text{-}6^+$ population as previously reported[7,8] (Figure S1B). Additionally, cynomolgus macaque pre-DCs were not detected using human Axl or Siglec-6 monoclonal antibody (mAb) (Figure S1C).

To further validate the identity of the cynomolgus macaque pre-DC subset in PBMCs, MHC-II expression was compared between pre-DCs and other DC subsets. In agreement with human studies, MHC-II expression on cynomolgus macaque pre-DCs was higher than on pDCs but lower than that of cDC2 (Figures 1E and S1D).

Additionally, we took advantage of the recently reported specific expression of TIGIT by pDCs relative to other cDC subsets in rhesus macaques.[45] TIGIT expression was also restricted to pDCs in cynomolgus macaques (Figures 1E and S1D). Furthermore, CD4 and CD81 receptors showed intermediate expression on cynomolgus macaque pre-DCs. These observations make them, along with TIGIT, additional markers for the discrimination of macaque pre-DCs from cDC1, cDC2, and pDCs (Figure S1D).

Pre-DC identity using our flow cytometry strategy was further validated by the intracellular expression of the proliferation marker Ki67. A high portion of pre-DCs defined by *Lin*$^-$/*CD123*$^+$/*MHC-II*$^+$/*Siglec-1*$^+$/*BDCA-2*^{low} showed intracellular expression of Ki67, whereas the majority of circulating pDCs among *Lin*$^-$/*CD123*$^+$/*MHC-II*$^+$/*Siglec-1*$^-$/*BDCA-2*$^+$ cells do not (Figure 1F). In contrast to pDCs, both cynomolgus macaque

(C) DC subsets, defined using the two different flow cytometry strategies described in (A) and (B) (CD33/CD45RA vs. CD123/Siglec-1), were compared on CD33 vs. CD45 FACS plots, with a color overlay of the pre-gated DC subsets. Frequencies of DC (live $CD45^+$ $MHC\text{-}II^+$ Lin^-) cells were quantified and compared using the different flow cytometry strategies presented in the graph.

(D) Representative flow cytometry strategy to identify circulating pre-DC in cynomolgus macaques: $CD123^+$ $Siglec\text{-}1^+$ $BDCA2^{low}$ pre-DC (red), $CD123^+$ $BDCA2^+$ $Siglec\text{-}1^-$ pDC (orange), $CD123^-$ $CADM1^+$ cDC1 (green), and $CD123^-$ $CD1c^+$ cDC2 (blue).

(E) Representative analysis of the expression level of MHC-II and TIGIT (MFI) on human and cynomolgus macaque circulating pre-DC (red) and pDC (orange). Histograms show one representative experiment out of six individuals.

(F) Analysis of Ki67 expression in macaque pre-DC (red) and pDC (orange) and proportions of $KI67^+$ pre-DC (mpre-DC) and pDC (mpDC) among cynomolgus macaques (n = 8). Statistical Wilcoxon test was performed (p = 0.0078). Error bars depict SD.

(G) Frequency of human (n = 14) vs. macaque (n = 31) blood pre-DCs (hpre-DC and mpre-DC, respectively), or blood pDC (hpDC and mpDC) among the total DC subsets. The total number of DCs was calculated by adding the four subpopulations of isolated DCs. Statistical Mann-Whitney test was performed (pre-DC, p = 0.0217; pDC, $p < 0.0001$). Error bars depict SD.

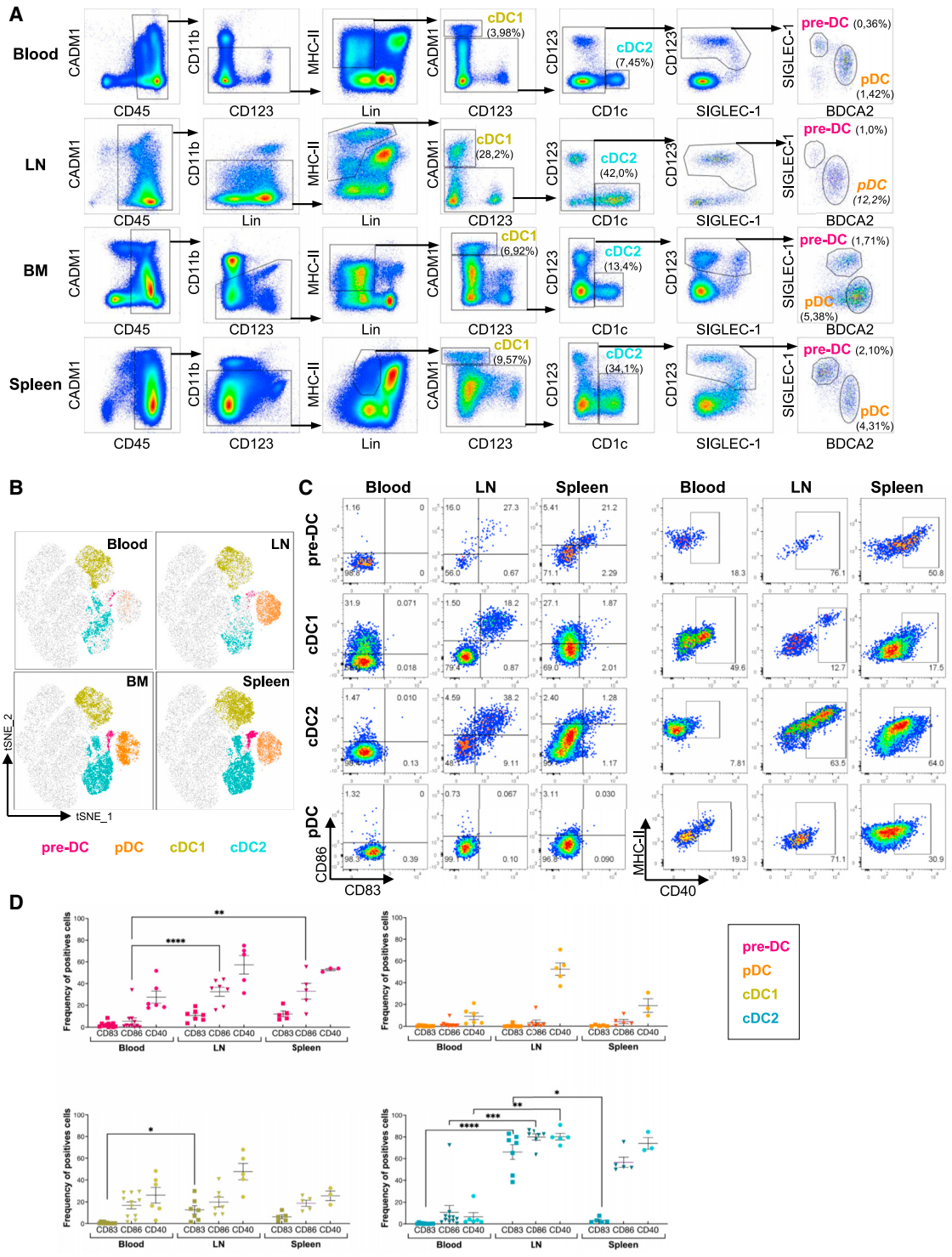

Figure 2. Characterization of pre-DC, pDC, and cDC across tissues in cynomolgus macaque

(A) Representative flow cytometry strategy Lin (CD3/CD8/CD14/CD20/CD34) to identify pre-DC, pDC, cDC1, and cDC2 from blood, peripheral lymph nodes (LNs), bone marrow (BM), and spleen of one representative cynomolgus macaque out of six. DC subsets were highlighted manually in each tissue: pre-DC (red), pDC (orange), cDC1 (green), and cDC2 (blue).

(B) Discrimination of the different DC subsets by unsupervised flow cytometry analysis in blood, LN, BM, and spleen of a representative cynomolgus macaque. All of the CD45^{+} MHC-II^{+} Lin^{-} (CD3/CD8/CD14/CD20/CD34) cells from the different tissues were isolated by manual gating and then concatenated into a unique t-SNE analysis. DC subsets were then highlighted in each tissue: pre-DC (red), pDC (orange), cDC1 (green), and cDC2 (blue).

(legend continued on next page)

and human pre-DC subsets expressed Ki67 (Figures 1F and S1E).

Frequency of circulating pre-DCs was then compared among PBMCs of cynomolgus macaques and humans. The frequency of circulating pre-DCs was slightly higher in cynomolgus macaques (mpre-DCs) than in humans (hpre-DCs) (Figure 1G). Meanwhile, circulating pDC frequencies were aligned with a previous study, with macaque PBMCs containing lower levels than human PBMCs.[46] In both species, pre-DC frequencies were much lower than pDC.

Additional studies have identified resting-state pre-DC from BM mononuclear cells (BMMCs), skin, and secondary lymphoid organs.[47–50] To determine if cynomolgus macaque pre-DCs retained their phenotype (*Lin*$^{-}$*/CD123*$^{+}$*/MHC-II*$^{+}$*/Siglec-1*$^{+}$*/BDCA-2*^{low}), other tissues (lymph node myeloid cells [LNMCs), splenocytes, and BMMCs) were also analyzed for the presence of pre-DCs and other DC subsets (Figures 2A and S2). Our strategy clearly identified pre-DCs within these different cynomolgus macaque tissues. Unsupervised t-distributed stochastic neighbor embedding (t-SNE) analysis (using MHC-II, CD123, Siglec-1, BDCA-2, CD1c, CADM1, and CD11b) and a manual gating overlay of pre-DC (red), pDC (orange), cDC1 (green), and cDC2 (blue) confirmed pre-DC identity by their independent clustering from pDC and cDC subsets in all tissues analyzed (Figure 2B). In addition, pre-DCs from different tissues always clustered in the same distinct t-SNE island, confirming consistent marker expression between the different tissues during the resting state.

Overall, these results identified human-equivalent pre-DCs in cynomolgus macaque to be *Lin*$^{-}$*MHC-II*$^{+}$*CD123*$^{+}$*Siglec-1*$^{+}$*BDCA-2*^{low}*TIGIT*$^{-}$*CD4*^{low}*CD81*^{low}. However, a minimal-marker strategy (*Lin*$^{-}$*MHC-II*$^{+}$*CD123*$^{+}$*Siglec-1*$^{+}$*BDCA-2*^{low}) can be applied efficiently across different tissues to discriminate pre-DCs from pDCs and other cDC subsets.

Differential expression of costimulatory molecules according to tissue localization and DC cytokine production upon TLR agonist stimulation by cynomolgus macaque pre-DCs

Using our validated pre-DC flow cytometry strategy, we interrogated the expression of costimulatory molecules and the production of DC cytokines by macaque DC subsets during resting state or after TLR stimulation.

During resting state, co-expression of CD83/CD86 costimulatory molecules on pre-DCs and cDC2s occurred either in the lymph node (LN) or spleen, but not in blood, while double-positive cDC1s were most abundant in the LN. In contrast, CD83/CD86-double-positive pDCs were not observed in these tissues (Figures 2C and 2D). Furthermore, CD40^{+} pre-DCs were present in secondary lymphoid organs and peripheral blood, alongside other CD40^{+} DC subsets (Figure 2D). Therefore, similarities and differences in costimulatory phenotype of pre-DCs occur across different tissues relative to other specific DC subsets during the resting state in healthy cynomolgus macaques.

The cytokine production capacity of pre-DCs upon TLR7/8 stimulation was compared to other DC subsets *ex vivo*. Similar to human pre-DCs,[7] cynomolgus macaque pre-DCs produced TNF-α and IL-12p40, but not interferon alpha (IFN-α), after incubation with R848 (Figures 3A and 3B); a much greater proportion of the pre-DC subset produced IL-12p40. In contrast, cynomolgus macaque pDCs produced IFN-α after R848 stimulation. Moreover, TNF-α production was observed only by cDC1, after stimulation with poly(I:C) and by monocytes after stimulation with lipopolysaccharide (LPS) (Figures 3A and S3A and S3B). The frequency of IL-12p40 and TNF-α producing pre-DCs was lower than that of pDCs from PBMCs and BMMCs, whereas their frequency in LNMCs was not significantly different (Figure 3B).

Overall, these data demonstrate that cynomolgus macaque pre-DCs share similarities with their human counterparts in the shared antigen-presenting phenotype and ability to produce DC cytokines when activated. These results also indicate that macaque pre-DCs may be directly involved in orchestrating immune responses to pathogens.

Circulating pre-DCs decrease in blood and accumulate in LN during early SIV infection

We performed a longitudinal study of pre-DC dynamics in PBMCs and lymphoid tissue of SIV-infected cynomolgus macaques (n = 12) (Figure 4A). In the chronic stage, six cynomolgus macaques were treated by anti-retroviral treatment (ART), whereas six were not (Figures 4A and 4B). Early acute increases of viral load were observed to mark the primary infection phase, peaking at day 10 ($\sim 10^7$ RNA copies/mL). Viral load reached a plateau around day 35 to define the chronic phase, which continued until the end of the study. The treatment with ART, from day 182 of chronic phase, elicited a rapid decrease of viral loads, plummeting to the detection threshold within 7 days, until the end of the study. The frequency of CD4^{+} T cells was also monitored in blood. An abrupt decrease in CD4^{+} T cells was elicited by SIV infection, followed by a continuous progressive decline during the course of the chronic phase (Figure 4C).

Concomitant with the peak of blood viral load, the absolute number of pre-DCs in PBMCs dropped significantly (non-infected [NI] vs. day 10 post-infection [p.i.] [D + 10]; p = 0.0001) (Figure 4D), while the proportion of pre-DCs increased in LNMCs (p = 0.0005) (Figure 4E). During chronic phase, a partial recovery of pre-DC in PBMC was observed (D + 10 vs. chronic; p = 0.0046) (Figure 4D), while a persistent increase of pre-DCs occurred in LNMCs (NI vs. D + 10; p = 0.003 and NI vs. chronic; p = 0.045) (Figure 4F). The decrease of pre-DCs in blood and their accumulation in LN also correlated with viral load

(C) Expression of costimulatory molecules CD86, CD83, and CD40 on pre-DC, pDC, cDC1, and cDC2 subsets from a representative uninfected cynomolgus macaque in blood, LN, and spleen.

(D) Frequencies of pre-DC, pDC, cDC1, and cDC2 subsets expressing the costimulatory molecules CD83, CD86, and CD40 in uninfected cynomolgus macaques in blood (n = 11 for CD83 and CD86 expression, n = 6 for CD40 expression), LN (n = 7 for CD83 and CD86 expression, n = 5 for CD40 expression), and spleen (n = 5 for CD83 and CD86 expression, n = 3 for CD40 expression); p values calculated by Mann-Whitney test: *p < 0.05, **p < 0.005, ***p < 0.0005, ****p < 0.0001. Error bars depict SD.

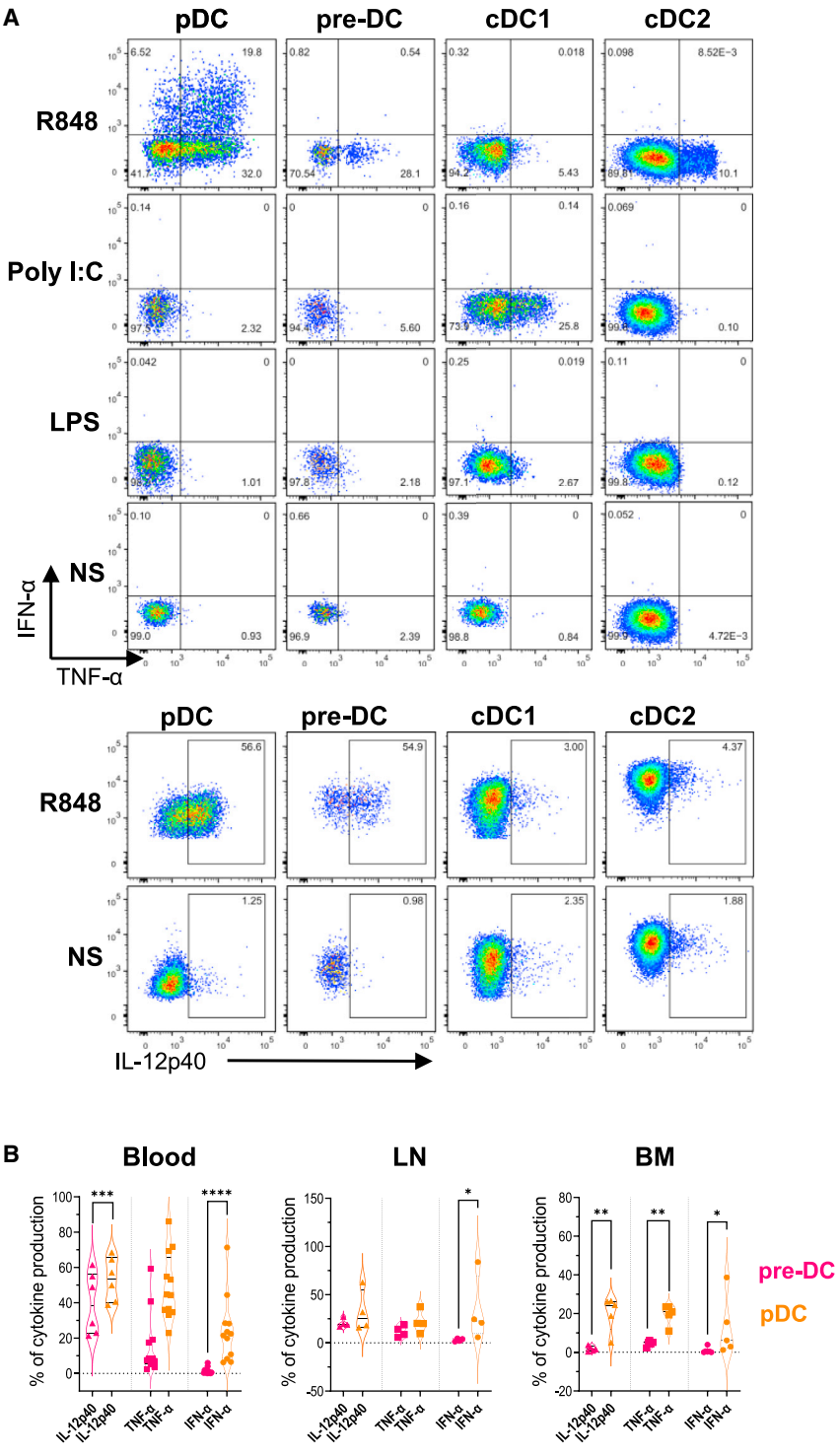

Figure 3. Characterization of pre-DC, pDC, cDC1, and cDC2 intracellular cytokine production after *ex vivo* TLR stimulation

(A) Dot plots of TNF-α, IFN-α, and IL-12p40 production by pDC, pre-DC, cDC1, and cDC2 in the blood of a representative uninfected cynomolgus macaque upon TLR stimulation. The cytokine production was measured by intracellular flow cytometry and dot plots show TNF-α and IFN-α production (up) after either TLR7/8 (R848), TLR3 (poly(I:C)), or TLR4 (LPS) stimulation or without stimulation (NS). IL-12p40 production (down) by DC subsets was assessed upon TLR7/8 (R848) stimulation or without stimulation (NS).

(B) Bar charts showing the frequency of cynomolgus macaque blood (n = 12), LN (n = 4), and BM (n = 5) pre-DCs (red) and pDCs (orange) producing IL-12p40, TNF-α, or IFN-α under TLR7/8 (R848) stimulation; p values calculated by Mann-Whitney test: *p < 0.05, **p < 0.005, ***p < 0.0005, ****p < 0.0001. Error bars depict SD.

(88.2%) and during the different phases of SIV infection (Figure 4G). In the acute phase of SIV infection, a slight decline in the proportion of blood Ki67$^+$ pre-DCs (day 3 = 80.4%; day 10 = 72.7%) was observed, with recovery during chronic phase (91.4%). In contrast, only 23.3% of pre-DCs expressed Ki67 in the LNs of uninfected animals (Figure 4H). This percentage increased significantly during acute phase and remained elevated during chronic phases (respectively, 49.4%, p = 0.01 and 45.7%, p = 0.01). The increased proportion of Ki67$^+$ pre-DC in LN strongly suggests that blood pre-DCs are rapidly recruited into the LN after SIV infection and that recruitment of pre-DCs to LN is sustained over the course of infection.

For comparison, cDC1, cDC2, and pDC dynamics were also evaluated over the same course of time (Figure S5). Concordant with previous studies,[39,43,51] both pDC and cDC2 numbers rapidly decreased in PBMCs of infected animals during acute SIV infection and also accumulated in LN, with a trend not unlike pre-DC dynamics (Figures S5A–S5C). Since CCR7 is a DC marker of homing to secondary lymphoid organs, we analyzed its expression on pre-DCs and pDCs from additional uninfected and SIV-infected animals (Figure S6). Our data showed a higher trend in CCR7 expression on LN pre-DCs compared to blood pre-DCs. However, no difference in CCR7 expression was observed between pre-DCs from uninfected and SIV-infected cynomolgus macaques, suggesting that the accumulation of pre-DCs in the LN (Figures S4A and S4B). In addition, these pre-DC dynamics correlated with those of cDC2 (Figure S4C).

Analysis of proliferation marker Ki67 by pre-DCs in PBMCs and LNMCs was also performed during the course of SIV infection. Most blood pre-DCs expressed Ki67 in uninfected animals

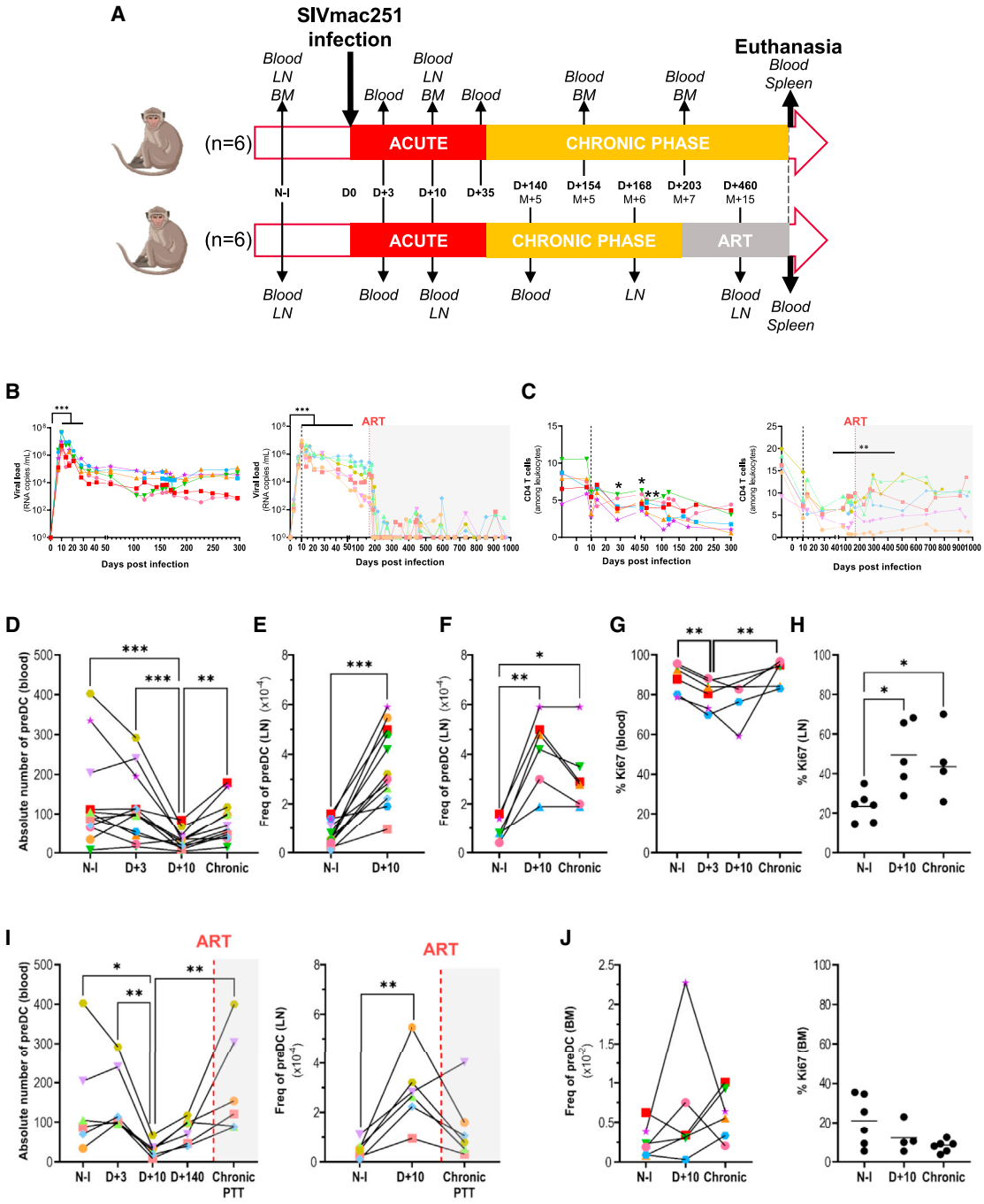

Figure 4. Analysis of the dynamics of cynomolgus macaque pre-DC at different stages of SIV infection

(A) Schematic representation of the study design. Follow-up of two groups of six cynomolgus macaques infected by SIVmac251 implemented or not with antiretroviral treatment (ART) after 26 weeks of infection. Tissues were sampled and analyzed before and during the follow-up of SIV infection.

(B) Follow-up of plasmatic viral load of the animals untreated (left, n = 6) or under ART (right, n = 6); p values calculated by Friedman test: ***p < 0.0005.

(C) Follow-up of the absolute count of blood $CD4^+$ T cells by flow cytometry analysis during SIV infection of animals untreated (left, n = 6) or under ART (right, n = 6); p values calculated by Friedman test: **p < 0.005 and *p < 0.05.

(D) Evolution of blood pre-DC absolute count per milliliter of blood during the follow-up of the two groups of cynomolgus macaques before treatment (n = 12); p values calculated by Friedman test: **p < 0.005 and ***p < 0.0005.

(E) Evolution of pre-DC frequency among $CD45^+$ leukocytes in LNs before (NI) and 10 days after SIV infection in the two groups of cynomolgus macaques (n = 12); p values calculated by Wilcoxon test: ***p = 0.0005.

(legend continued on next page)

could result from an alteration in their capacity to differentiate into cDCs.

Additionally, ART elicited a significant recovery of pre-DCs in PBMCs (Figure 4I), while significant decreases in frequency were observed in LNMCs, to restore levels observed in uninfected animals (Figure 4I right vs. 4F).

ART also affected other DC dynamics, but differently (Figures S5B–S5D). PBMC pDCs increased after treatment (Figure S5B right), while pDCs in LNMCs decreased but failed to reach parity with uninfected levels in LNMCs (Figure S5E right). In the blood, the effects of ART on cDC1 and cDC2 may not have been noticeable (Figure S5B), but frequencies in LNMCs rose after ART (Figure S5E). Thus, ART normalizes pre-DC and pDC dynamics, whereas little impact was observed in cDC1 and cDC2 dynamics in chronic SIV-infected animals.

Due to the observed decline of circulating pre-DC numbers in PBMCs during early SIV infection (Figures 4D and 4I), we postulated that an ''emergency hematopoiesis state'' may arise in the BM niche to compensate for this loss. While only subtle decreases in BMMC pre-DC frequency may have occurred during early SIV infection, greater increasing trends occurred from acute infection into chronic phase, leaving BMMC pre-DC frequencies elevated during chronic phase (Figure 4J). However, the Ki67$^+$ proportion of these BMMCs pre-DCs seemed to decline from acute to chronic infection phase, suggesting that there may be a deficiency in the ability to replenish proliferating pre-DCs in BM over the course of SIV infection (Figure 4J right). Even though pre-DCs were ever present among PBMCs and BMMCs over the course of SIV infection (Figures 4G and 4J), the decline of Ki67$^+$ pre-DCs in BM suggests that chronic infection with SIV could eventually exhaust the BM pre-DC compartment (Figure 4J right).

Altogether, our data demonstrated the dynamics of pre-DCs during SIV infection, declining in blood early during acute infection and increasing in LN, likely due to their recruitment from the periphery. During the chronic phase, pre-DCs only partially recovered in blood, while recruitment to LN persisted. However, ART reversed pre-DC accumulation in LN, and possibly also in blood, returning to NI levels.

SIV infection impairs LN pre-DC functionality

The activation phenotype (CD83, CD86, and MHC-II) of pre-DCs from PBMCs, LNMCs, or spleen was assessed during the different phases of SIV infection. It is expected that pre-DCs in blood would be exposed to virus, due to high viral loads detected during primary infection phase. While an activated phenotype was expected, CD83, CD86, and MHC-II were not increased on blood pre-DCs during acute infection or during the chronic phase (Figure 5A). In LN, pre-DCs significantly increased CD83 and CD86 expression, but only during the chronic phase (Figure 5B). Furthermore, MHC-II expression appeared downregulated during acute-phase infection, to partially rebound during chronic phase. In contrast, other circulating DC subsets did not upregulate costimulatory molecules during SIV infection (Figure S7). Moreover, analysis of additional animals (n = 3) did not identify downregulation of MHC-I molecules on DC subsets during SIV infection (Figure S8).

The spleen is a major secondary lymphoid organ, functioning to facilitate adaptive immune response initiation via promotion of DC-T cell interactions. While spleens were not accessible during early infection, they were harvested at euthanasia of chronically infected animals (Figure 5C). CD83 expression on spleen pre-DCs during chronic SIV infection was significantly higher than in spleen pre-DCs from NI cynomolgus macaques.

We also analyzed the expression of the CD95 marker in additional (n = 2) infected animals, which is associated with activation and apoptosis on pre-DCs (Figure S9). Upregulation of CD95 on circulating pre-DCs was triggered by SIV infection, with over 70% expressing high levels during all phases of SIV infection. At day 10 p.i., 100% of pre-DCs from PBMCs or LN expressed even higher levels of CD95, suggesting their activation or susceptibility to apoptosis at the peak of infection.

DCs can sense SIV and HIV through pattern-recognition receptors, including endosomal TLR7 and 8, which sense single-stranded RNA (ssRNA) and activate MyD88-dependent signaling pathways for the production of IFN-I and inflammatory cytokines. We monitored the pre-DC TLR7/8-dependent response, *ex vivo* in bulk PBMCs or LNMCs, by using R848 (synthetic dual TLR7/8 agonist) to mimic ssRNA TLR7/8 targeting. Intracellular expression of IL-12p40, TNF-α, and IFN-α were quantified (Figure 6A). A higher proportion of IL-12p40- and TNF-α-producing pre-DCs was transiently observed in the blood at the peak of infection, 10 days p.i., compared to NI animals ($p = 0.03$ and $p = 0.003$, respectively), (Figure 6B).

In contrast, the capacity of pre-DCs from LN to produce IL-12p40 was severely attenuated (NI, 20.33% ± 2.25% vs. D + 10 5.36% ± 1.37%, $p = 0.045$; and NI vs. chronic, 2.33% ± 1.28% $p = 0.007$) during early and chronic SIV infection phases (Figure 6C). Meanwhile, LN pre-DCs' ability to produce TNF-α was almost not affected.

Production of IFN-α was barely detected from R848-stimulated PBMCs or LN pre-DCs (Figure 6A). In contrast, and as expected, stimulation of PBMC- or LN-derived pDCs with R848 elicited robust production of IFN-α (Figure S10); higher frequencies of IFN-α-producing blood pDCs were detected

(F) Follow-up of pre-DC frequency among CD45$^+$ leukocytes in LNs before infection (NI) and during acute (D + 10) and chronic phase of SIV infection (n = 6); p values calculated by Friedman test: *$p < 0.05$ and**$p < 0.005$.

(G and H) Analysis of pre-DC proportion expressing Ki67 in the blood (G, n = 6) and peripheral LNs (H) before (NI, n = 6) and at different times after SIV infection (D + 10, n = 5; chronic, n = 4); p values calculated by Friedman test (G) **$p < 0.005$ and by Kruskal-Wallis test (H) *$p < 0.05$.

(I) Impact of ART implementation (red dotted line) on the absolute number of pre-DC per milliliter of blood (left) and on the frequency of pre-DCs among CD45$^+$ leukocytes in LNs (right) (n = 6). The chronic phase after treatment (chronic post-treatment [PTT]) is shown in gray background. Blood and LNs were collected during the chronic phase of infection, after 9 weeks of treatment; p values calculated by Friedman test: **$p < 0.005$, *$p < 0.05$.

(J) Frequency of pre-DCs among leukocytes from BM and proportion of Ki67$^+$ pre-DCs during SIV infection (n = 6). Friedman test (left) and Kruskal-Wallis test (right) were performed. NI, and chronic corresponds to 8 months post SIV infection.

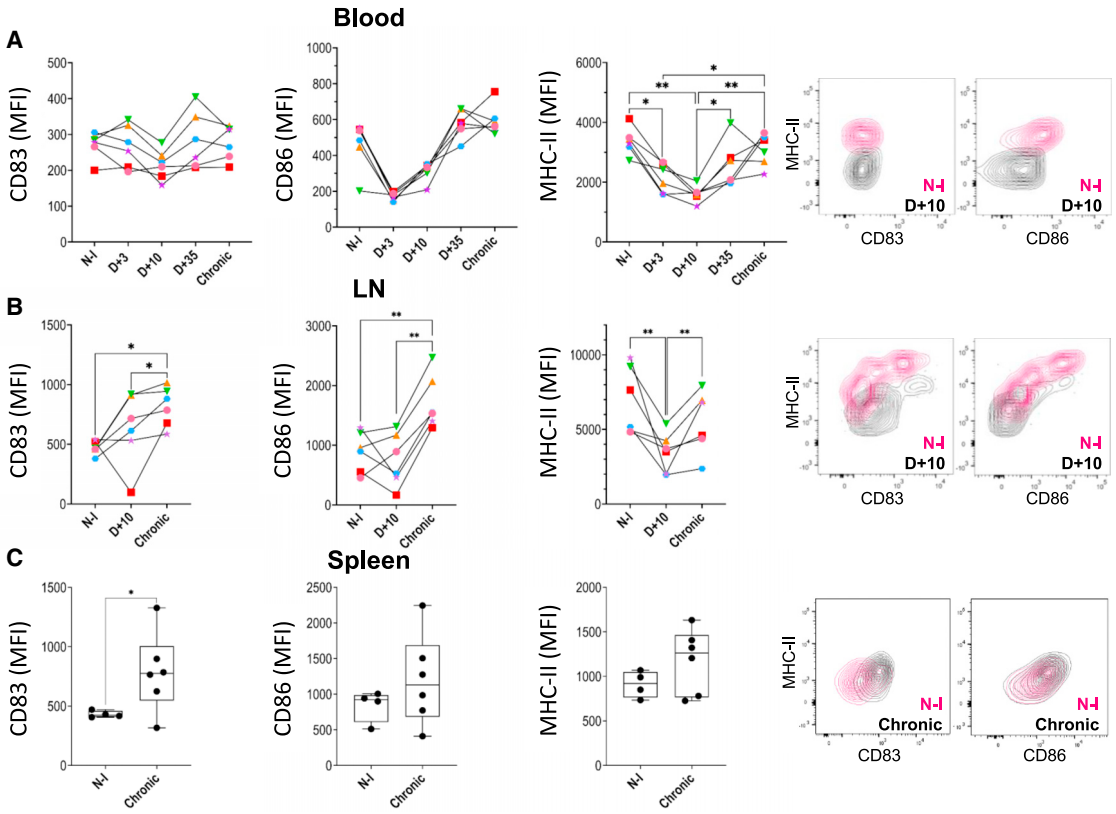

Figure 5. Follow-up of costimulatory molecules and MHC-II expression on pre-DC during SIV infection

Expression level of costimulatory molecules (CD83, CD86, and MHC-II) on pre-DCs during the follow-up of the animals in (A) blood (n = 6), (B) LN (n = 6), and (C) spleen (NI, n = 4 vs. chronic [8 months post infection], n = 6). Contour plots of CD83, CD86, and MHC-II expression on pre-DC in blood, LN, and spleen from a representative cynomolgus macaque before (red) and 10 days after (black) SIV infection are shown; p values calculated by Friedman test (A and B), *p < 0.05, **p < 0.005; and by Kruskal-Wallis test (C), *p < 0.05. The results are represented as MFI.

when harvested at the peak of infection (day 10 p.i.), whereas less LN pDC produced IFN-α in chronic phase. However, the capacity of pDC to produce TNF-α or IL-12p40 under TLR7/8 stimulation was not significantly modified by SIV infection status (Figure S10).

Overall, these data indicate that SIV infection alters pre-DC functionality early during SIV infection by inhibition of costimulatory and MHC-II molecule expression and disabling production of IL-12p40 in LN upon TLR7/8 stimulation.

Circulating human pre-DCs decrease during primary HIV infection

Human blood pre-DCs were characterized by flow cytometry from (1) NI (NI) donors (n = 16), (2) HIV primary infection (primo) of PLWH (n = 19) longitudinally sampled at inclusion and after 1 year of effective ART, and (3) people who are termed elite controllers (ECs) that naturally control HIV replication (n = 10) (Figure 7). Clinical parameters of PLWH are shown in Table S1. Pre-DCs, cDC1s, cDC2s, and pDCs were defined from PBMCs; pre-DCs were defined as MHC-II$^+$ CD141$^-$ CD123$^+$ AXL$^+$ (Figure S11A). This DC subset experienced a decrease (p = 0.03) during primary HIV infection (NI 1.06% ± 0.57% vs. Primo 0.66% ± 0.47%), as observed in the SIV model, while ART seemed to replenish the pre-DC pool (1.93% ± 1.59%) (Figure 7A). A similar effect was observed for the other DC subsets (Figure 7A), with lower frequencies during primary HIV infection, and improving with ART; almost all PLWH responded to ART with increased frequencies of cDC1 (p < 0.0001) and pDC (p = 0.0003) in the blood. We also analyzed recently discovered DC3 subsets that play an important role in the shaping of CD8 T cell responses. The frequency of DC3 subsets decreased in primary HIV infection and increased following ART administration, regardless of CD14 and CD163 expression (Figures S11B and S11C). In addition, the frequency of the CD163$^-$/CD14$^-$ subset of DC3 was significantly higher in ECs than in the other groups.

We further investigated whether HIV infection status influenced the maturation state of blood pre-DCs. Expression of costimulatory molecules (CD40, CD80, CD86, and CD83) on the surface of pre-DCs were compared between PLWH groups. CD86 was expressed by most pre-DCs (Figure 7C) as expected, regardless of the infectious state (NI, 72.1% ± 12%; Primo, 68.8% ± 13%; ART, 66.2% ± 15.2%; EC, 81.5% ± 9.9%), except a higher mean fluorescence intensity (MFI) trend was observed for ECs. Smaller proportions of pre-DCs expressed CD40 (~14%), CD80 (~4.8%), or CD83 (~8.5%), regardless of the

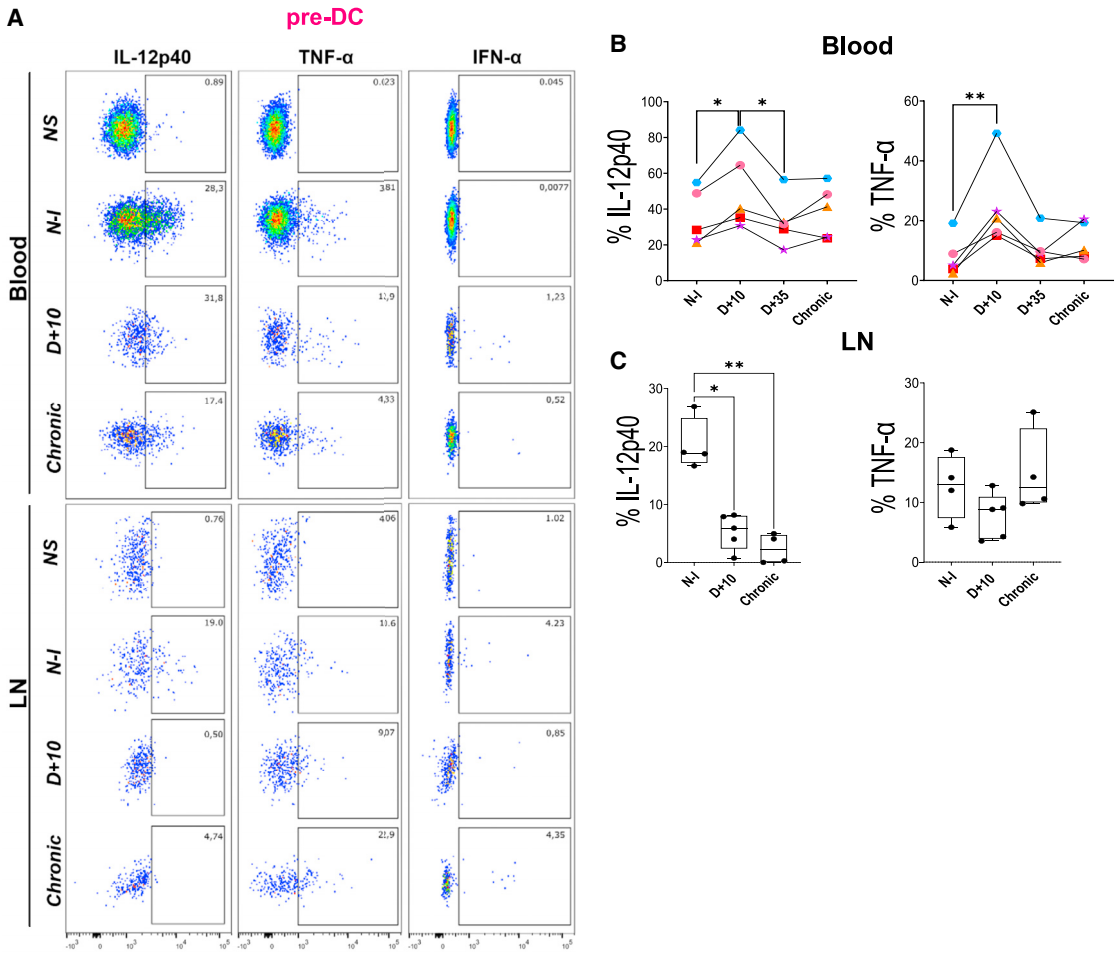

Figure 6. Analysis of IL-12p40 and TNF-α production following TLR7/8 stimulation of pre-DC from SIV-infected cynomolgus macaques

(A) Intracellular flow cytometry analysis of blood (up) and LNs (down) pre-DC stained for TNF-α, IL-12p40, and IFN-α expression after R848 *ex vivo* stimulation, or not (NS), from a representative cynomolgus macaque before infection (NI) and at D + 10 and in chronic phase of SIV infection. Unstimulated controls correspond to the baseline sample of one representative cynomolgus macaque. Pre-DCs were gated by flow cytometry analysis and intracellular production of IL-12p40, TNF-α, or IFN-α after 3 h of *ex vivo* stimulation by R848 (1 μg/mL), including incubation with Brefeldin A for the last hour, at different time points of SIV infection. (B and C) Intracellular flow cytometry analysis of the proportion of (B) blood (n = 6) or (C) LN pre-DCs (NI, n = 4; D + 10, n = 5; chronic, n = 4) producing IL-12p40 or TNF-α during SIV infection. Pre-DCs were gated by flow cytometry analysis and intracellular production of IL-12p40 and TNF-α after 3 h of *ex vivo* stimulation by R848, including incubation with Brefeldin A for the last hour, at different time points of SIV infection; p values calculated by Friedman test (blood; *$p < 0.05$ and **$p < 0.005$) and by Kruskal-Wallis test (LN; *$p < 0.05$ and **$p < 0.005$).

infectious state. Expression of these costimulatory molecules on pre-DCs was not significantly affected by HIV infection status or following administration of ART (Figure 7C). However, analysis of EC samples showed that the level of expression of costimulatory molecules (CD40, CD80, CD86) on pre-DCs was associated with the level of $CD4^+$ and $CD8^+$ T cell activation (Figure 7D). Analysis of cDC1, cDC2, and pDC subsets in EC samples also showed some correlations between costimulatory molecules expression and the level of T cell activation but to a lesser extent than pre-DC (Figure S12).

These results in PLWH reflect our results from pre-DCs in the cynomolgus macaque model of SIV infection to show a sharp decrease in circulating pre-DC abundance also occurring during early HIV-1 infection in PLWH. Moreover, a strong correlation between expression of costimulatory molecules on pre-DCs and the activation of T cells in EC individuals, who naturally control HIV replication, was identified.

DISCUSSION

Herein, we report the characterization of human pre-DC equivalents in cynomolgus macaques and their dynamics during SIV and corresponding HIV infection in PLWH. The study of pre-DCs following HIV infection is highly relevant due to their specific expression of the HIV receptor, Siglec-1.[38] Since pre-DCs possess DC-like functionality and are recruited to sites of infection, it is of high importance to determine their dynamics of recruitment into secondary lymphoid organs and whether

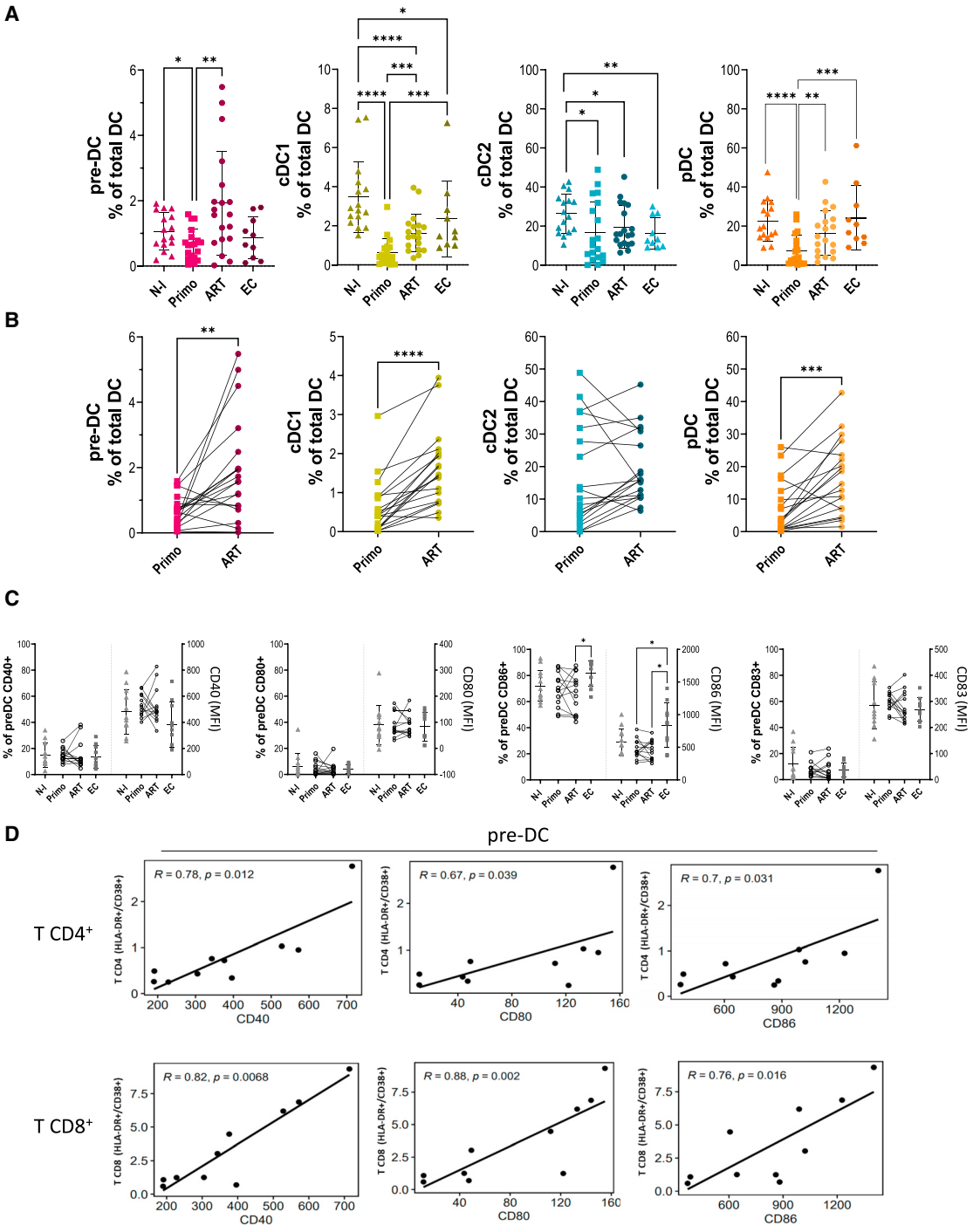

Figure 7. Analysis of circulating pre-DCs in people living with HIV

(A and B) Proportion of circulating pre-DC, cDC1, cDC2, and pDC among Lin^{neg}/HLA-DR^{high} in NI donors (NI, n = 16) in primary HIV infection of PLWH (Primo, n = 19), PLWH under ART (ART, n = 19), and elite controllers (ECs, n = 10). The amounts of each DC subset were compared between the different groups (A) and a longitudinal analysis between samples of PLWH during primary infection and after 1 year of effective ART was carried out (B). p values calculated by Mann-Whitney test (A) and by Wilcoxon test (B): *p < 0.05, **p < 0.005, ***p < 0.005, ****p < 0.0001. Error bars depict SD.

(C) Human circulating pre-DCs were analyzed for the expression of CD40, CD80, CD86, and CD83 represented either as percentage of positive cells or MFI of the different markers; p values calculated by Mann-Whitney test: *p < 0.05. Error bars depict SD.

(D) Correlation analysis between the expression of costimulatory molecules on pre-DCs and the level of CD4$^+$ and CD8$^+$ T cell activation in ECs. Positive correlation between CD40, CD80, and CD86 levels on pre-DCs and activation of CD4$^+$T cells (left) or CD8$^+$ T cells (right) determined by surface co-expression of CD38 and HLA-DR markers. The Spearman R correlation coefficient and p values are shown on each plot.

changes in their activation phenotype and effector functions would be induced following HIV infection.

To overcome difficulties in accessing the secondary lymphoid organs of PLWH early during infection, we used the cynomolgus macaque SIV infection model, which displays similar pathogenesis to human disease. The macaque model has already been useful in defining the dynamics and functions of pDCs and cDCs during SIV infection.[42,43,51–53] Even though the cynomolgus macaque SIV infection model of HIV infection in people is outstanding for studies that interrogate very early immune responses to HIV, and the inclusion of peripheral tissue sampling, discrepancies in the identification of some key markers for human DC equivalents are present (including CD141 and CD11c).[54–56] We first characterized the equivalent of human pre-DCs in cynomolgus macaques, as a method for their identification and isolation was not yet available. We found that some human-equivalent pre-DC markers were not suitable in macaques, such as CD33 and CD45RA. Along this line, a previous study reported that human and mouse pre-DCs are distinguished through different markers.[49]

Therefore, we developed a multiparameter flow cytometry strategy to unambiguously isolate human-equivalent macaque pre-DCs from other DC subsets across tissues, which we then used to study pre-DCs from blood and secondary lymphoid organs after SIV infection. A combination of common surface markers shared between macaque and human pre-DCs was identified, including CD123, Siglec-1, BDCA-2, and MHC-II. Our study identified additional markers such as TIGIT, CD4, and CD81 that are also suitable to distinguish pre-DCs from other DC subsets in cynomolgus macaques, equally applicable in human studies. Moreover, we showed that such defined pre-DCs produced IL-12p40 and TNF-α, but not type-I IFN, upon TLR7/8 stimulation in both species.

This characterization identified a decrease in circulating pre-DCs during early SIV infection, associated with an increased proportion of pre-DCs in LN of SIV-infected animals. This may reflect their migration from blood into secondary lymphoid organs, as we previously reported for pDCs in the same SIV model,[43] or into sites of infection as observed in the lungs of mice during influenza infection.[49,57,58] In favor of this hypothesis, the proportion of Ki67-expressing pre-DCs, which was high at baseline in the blood and low in LN, nearly doubled in LN during early and chronic SIV infection. These profound increases were tempered by ART, suggesting that active SIV infection is directly responsible for the changes in pre-DC dynamics in the blood and LN. Furthermore, the proportion of Ki67$^+$ pre-DCs dropped drastically in BM over the course of chronic SIV infection, suggesting that the exit of pre-DCs from BM is also involved in these dynamics, likely responsible for the progressive restoration of pre-DC numbers and optimal Ki67 expression in the blood in the chronic stage.

On the other hand, loss of circulating pre-DCs during early SIV infection could also result from apoptosis mechanisms or even be triggered by a bystander response to the inflammatory environment elicited by SIV infection, as previously reported for other DC subsets.[59,60] In either case, pre-DCs upregulated death receptors during SIV infection, as observed with CD95. Thus, instead of proliferating and maturing to replenish cDC numbers, they may be dying. However, given that CD95 is also induced on activated cells, analysis of further apoptosis markers will be required.

Pre-DCs display an immature DC phenotype or are delayed in activating in response to SIV, which also has been reported for cDCs in the chronic phase of SIV infection.[61] This was observed in our study by their apparent non-activated blood phenotype, lack of CD86 expression in LN, and significantly decreased MHC-II expression profile. The lack of costimulatory molecules and downregulated MHC-II, instead of being upregulated, may be a hallmark of pre-DC functional inhibition by SIV, leading to poor viral antigen presentation to T cells, thereby weakening adaptive immune responses to SIV/HIV.

In line with this hypothesis, LN pre-DCs massively lost their ability to produce IL-12p40 early in SIV infection, although a slight increase of TNF-α and IL-12p40 was transiently observed in the blood. It is well established that IL-12 is a major factor for induction of Th1 differentiation and is also an activator of natural killer (NK) cell anti-viral function.[62,63] Therefore, the pre-DC deficiency in capacity to produce IL-12 in lymphoid tissues could represent a mechanism of SIV/HIV-mediated immune dysregulation, like that observed for other antigen-presenting cells.[53,64,65] Future studies characterizing IL-12 and other cytokine production from different DC subsets, in parallel, will be important to better understand how viral infection specifically affects each subset in secondary lymphoid organs.

Chronic latent SIV or HIV infection of different DC subsets remains a subject of debate. Recent *in vitro* studies demonstrated that pre-DCs were susceptible to HIV infection due to the expression of Siglec-1, to a greater extent than other DC subsets.[37,38] The identification of cynomolgus macaque pre-DC human equivalents enables future studies aiming to characterize their infection *in vivo* and implications arising from them being the viral reservoir.

Analysis of pre-DCs, and other DCs, in the blood of PLWH confirmed their loss during primary phase of HIV infection, as in the SIV model. However, ART did not elicit significant changes in costimulatory molecule expression on DC subsets. By comparison to the SIV model, this loss in blood could correspond to losses in the BM and sustained accumulation of pre-DCs in LN. Therefore, replenishment of pre-DC numbers in blood of PLWH under ART may result from the control of HIV infection in pre-DCs corresponding to a rejuvenation of dividing pre-DCs in BM, contraction of sustained pre-DC accumulation in LN, so that they may differentiate to replenish cDC subsets. Increases in DC3 subsets, an important subset for eliciting CD8 T cell responses,[66] were also observed after ART to match numbers in ECs who have effective anti-HIV CD8 T cell responses.[67] Our study also demonstrated a strong correlation between the expression of costimulatory molecules on pre-DCs and the level of T cell activation in spontaneous HIV controllers. In this respect, it would be highly relevant to use the SIV model in future studies to assess the impact of changes in pre-DCs in LNs on adaptive immune responses, in particular on the priming magnitude and functionality of virus-specific CD8$^+$ T cells.

Limitations of the study

Although our study identifies equivalent of human pre-DCs in cynomolgus macaque and provides evidence of their dysregulation

following SIV infection, several limitations should be mentioned. Pre-DCs are very rare, and the amount of blood and LNs sampled during our study was limited for ethical reasons. Consequently, we could not sort macaque pre-DCs to more deeply characterize their properties (to assess their capacity to stimulate T cell responses) or to differentiate them into functional cDC1s or cDC2s *ex vivo* before or after SIV infection. In addition, due to the difficulty of obtaining sufficiently purified cells, such a study would require a combination of culture medium conditions, cytokines, and/or stromal cells suitable for the differentiation and survival of macaque pre-DC *in vitro*, which are currently undefined. Additionally, we were unable to determine whether modifications of pre-DCs during SIV infection were caused by viral sensing and/or by inflammatory mechanisms induced by the infection. The gut constitutes an important reservoir of HIV replication[68] and pre-DCs were recently found in this tissue in mice.[69] While we attempted to analyze this tissue compartment, the number of total DCs from these samples was too low to unambiguously study pre-DCs. In addition, enzymatic treatment of gut samples being needed for cell isolation could alter pre-DC phenotypes and preclude their functional study.

Conclusions

Considering that pre-DCs are more susceptible to HIV-1 infection than other DC subsets *in vitro*, it is likely that the infection of pre-DCs during early acute infection, persisting during chronic phase, could be particularly important in HIV pathophysiology. Future studies using single-cell spatial transcriptomic approaches will be important in addressing these key questions to foster our understanding of how viral infection regulates pre-DCs in secondary lymphoid organs and the subsequent consequences on shaping adaptive immune responses to HIV.

In summary, this study identified human-equivalent pre-DCs in a preclinical model of HIV infection to demonstrate that pre-DC dysregulation may affect the development of effective anti-viral immune responses. These findings have direct implications on the pathophysiology caused by HIV in PLWH. Future studies aiming to characterize the impact of this dysregulation on disease progression, and also the contribution of pre-DCs from tissues as a viral reservoir, will be crucial for the design of new therapeutic strategies against HIV.

STAR★METHODS

Detailed methods are provided in the online version of this paper and include the following:

- KEY RESOURCES TABLE
- RESOURCE AVAILABILITY
  - Lead contact
  - Materials availability
  - Data and code availability
- EXPERIMENTAL MODEL AND STUDY PARTICIPANT DETAILS
- METHOD DETAILS
  - SIV infections & sample collection
  - SIV viral load quantification
  - Tissues processing
  - Antibody staining of cells & flow cytometry analysis
  - TLR agonist stimulation *ex vivo* & intracellular cytokine staining
- QUANTIFICATION AND STATISTICAL ANALYSIS

SUPPLEMENTAL INFORMATION

Supplemental information can be found online at https://doi.org/10.1016/j.celrep.2024.113994.

ACKNOWLEDGMENTS

We thank the staff of the animal facility of IDMIT, particularly Q. Sconosciuti, B. Delache, M. Pottier, S. Langlois, J.M. Robert, and N. Dhooge. We would like to thank F. Abdallah for her help with tissue processing and assistance with the experiments and K. Mulder and C. De La Calle Fabregat for data analysis. We also thank J. Van Wassenhove, M. Gomez Parcheco, W. Gros, and A.S. Gallouet for flow cytometry assistance and N. Bosquet, L. Bossevot, M. Leonec, L. Moenne-Loccoz, and J. Morin for the RT-qPCR assays. We thank the blood donors from the Établissement Français du Sang (EFS) and ANRS (French National Agency for AIDS research) CO6 PRIMO and CO21 CODEX cohort for helpful collaboration as well as Faroudy Boufassa, Laurence Meyer, and all the medical professionals involved in blood sampling at the Hôpital Kremlin-Bicêtre. This work was supported by the Programme Investissements d'Avenir (PIA), managed by the ANR under reference ANR-11-INBS-0008, funding the Infectious Disease Models and Innovative Therapies (IDMIT, Fontenay-aux-Roses, France) infrastructure, and ANR-10-EQPX-02-01, funding the FlowCyTech facility (IDMIT, Fontenay-aux-Roses, France), and the Agence Nationale de la Recherche sur le SIDA (ECTZ159192), and Sidaction (21-1-AEQ-12963). We thank Gilead and ViiV for providing the antiretroviral drugs. Animal studies were supported by the Agence Nationale de la Recherche sur le SIDA and MSDAVENIR, as part of the ANRS RHIVIERA pVISCONTI research program. The funders had no role in study design, data collection and analysis, decision to publish, or preparation of the manuscript. M.G. received a PhD scholarship from the University of Paris-Saclay and ANRS.

AUTHOR CONTRIBUTIONS

Conduct of experiments, M.G.; conceptualization, M.G. and B.F.; methodology, M.G., F.M., O.H., S.C., and B.V.; formal analysis, M.G. and B.F.; study management, B.F. and M.G.; provision of essential material, O.L., R.L.G., D.D., N.D., C.G., and F.R.; supervision, B.F.; writing of the original draft, B.F. and M.G.

DECLARATION OF INTERESTS

The authors declare no competing interests.

Received: April 14, 2023
Revised: January 27, 2024
Accepted: March 8, 2024
Published: March 25, 2024

REFERENCES

1. Cabeza-Cabrerizo, M., Cardoso, A., Minutti, C.M., Pereira da Costa, M., and Reis e Sousa, C. (2021). Dendritic Cells Revisited. Annu. Rev. Immunol. *39*, 131–166. https://doi.org/10.1146/annurev-immunol-061020-053707.
2. Collin, M., McGovern, N., and Haniffa, M. (2013). Human dendritic cell subsets. Immunology *140*, 22–30. https://doi.org/10.1111/imm.12117.
3. Merad, M., Sathe, P., Helft, J., Miller, J., and Mortha, A. (2013). The dendritic cell lineage: ontogeny and function of dendritic cells and their subsets in the steady state and the inflamed setting. Annu. Rev. Immunol. *31*, 563–604. https://doi.org/10.1146/annurev-immunol-020711-074950.

4. Cella, M., Jarrossay, D., Facchetti, F., Alebardi, O., Nakajima, H., Lanzavecchia, A., and Colonna, M. (1999). Plasmacytoid monocytes migrate to inflamed lymph nodes and produce large amounts of type I interferon. Nat. Med. *5*, 919–923. https://doi.org/10.1038/11360.

5. Breton, G., Lee, J., Zhou, Y.J., Schreiber, J.J., Keler, T., Puhr, S., Anandasabapathy, N., Schlesinger, S., Caskey, M., Liu, K., and Nussenzweig, M.C. (2015). Circulating precursors of human CD1c+ and CD141+ dendritic cells. J. Exp. Med. *212*, 401–413. https://doi.org/10.1084/jem.20141441.

6. Breton, G., Zheng, S., Valieris, R., Tojal da Silva, I., Satija, R., and Nussenzweig, M.C. (2016). Human dendritic cells (DCs) are derived from distinct circulating precursors that are precommitted to become CD1c+ or CD141+ DCs. J. Exp. Med. *213*, 2861–2870. https://doi.org/10.1084/jem.20161135.

7. See, P., Dutertre, C.A., Chen, J., Günther, P., McGovern, N., Irac, S.E., Gunawan, M., Beyer, M., Händler, K., Duan, K., et al. (2017). Mapping the human DC lineage through the integration of high-dimensional techniques. Science *356*, eaag3009. https://doi.org/10.1126/science.aag3009.

8. Villani, A.C., Satija, R., Reynolds, G., Sarkizova, S., Shekhar, K., Fletcher, J., Griesbeck, M., Butler, A., Zheng, S., Lazo, S., et al. (2017). Single-cell RNA-seq reveals new types of human blood dendritic cells, monocytes, and progenitors. Science *356*, eaah4573. https://doi.org/10.1126/science.aah4573.

9. Matsui, T., Connolly, J.E., Michnevitz, M., Chaussabel, D., Yu, C.I., Glaser, C., Tindle, S., Pypaert, M., Freitas, H., Piqueras, B., et al. (2009). CD2 distinguishes two subsets of human plasmacytoid dendritic cells with distinct phenotype and functions. J. Immunol. *182*, 6815–6823. https://doi.org/10.4049/jimmunol.0802008.

10. Altfeld, M., Fadda, L., Frleta, D., and Bhardwaj, N. (2011). DCs and NK cells: critical effectors in the immune response to HIV-1. Nat. Rev. Immunol. *11*, 176–186. https://doi.org/10.1038/nri2935.

11. Manches, O., Frleta, D., and Bhardwaj, N. (2014). Dendritic cells in progression and pathology of HIV infection. Trends Immunol. *35*, 114–122. https://doi.org/10.1016/j.it.2013.10.003.

12. Miller, E., and Bhardwaj, N. (2013). Dendritic cell dysregulation during HIV-1 infection. Immunol. Rev. *254*, 170–189. https://doi.org/10.1111/imr.12082.

13. Rhodes, J.W., Tong, O., Harman, A.N., and Turville, S.G. (2019). Human Dendritic Cell Subsets, Ontogeny, and Impact on HIV Infection. Front. Immunol. *10*, 1088. https://doi.org/10.3389/fimmu.2019.01088.

14. Coindre, S., Tchitchek, N., Alaoui, L., Vaslin, B., Bourgeois, C., Goujard, C., Lecuroux, C., Bruhns, P., Le Grand, R., Beignon, A.S., et al. (2019). Mass Cytometry Analysis Reveals Complex Cell-State Modifications of Blood Myeloid Cells During HIV Infection. Front. Immunol. *10*, 2677. https://doi.org/10.3389/fimmu.2019.02677.

15. Huang, J., Yang, Y., Al-Mozaini, M., Burke, P.S., Beamon, J., Carrington, M.F., Seiss, K., Rychert, J., Rosenberg, E.S., Lichterfeld, M., and Yu, X.G. (2011). Dendritic cell dysfunction during primary HIV-1 infection. J. Infect. Dis. *204*, 1557–1562. https://doi.org/10.1093/infdis/jir616.

16. Loré, K., Sönnerborg, A., Broström, C., Goh, L.E., Perrin, L., McDade, H., Stellbrink, H.J., Gazzard, B., Weber, R., Napolitano, L.A., et al. (2002). Accumulation of DC-SIGN+CD40+ dendritic cells with reduced CD80 and CD86 expression in lymphoid tissue during acute HIV-1 infection. AIDS *16*, 683–692. https://doi.org/10.1097/00002030-200203290-00003.

17. Sabado, R.L., O'Brien, M., Subedi, A., Qin, L., Hu, N., Taylor, E., Dibben, O., Stacey, A., Fellay, J., Shianna, K.V., et al. (2010). Evidence of dysregulation of dendritic cells in primary HIV infection. Blood *116*, 3839–3852. https://doi.org/10.1182/blood-2010-03-273763.

18. Bashirova, A.A., Martin-Gayo, E., Jones, D.C., Qi, Y., Apps, R., Gao, X., Burke, P.S., Taylor, C.J., Rogich, J., Wolinsky, S., et al. (2014). LILRB2 interaction with HLA class I correlates with control of HIV-1 infection. PLoS Genet. *10*, e1004196. https://doi.org/10.1371/journal.pgen.1004196.

19. Dillon, S.M., Friedlander, L.J., Rogers, L.M., Meditz, A.L., Folkvord, J.M., Connick, E., McCarter, M.D., and Wilson, C.C. (2011). Blood myeloid dendritic cells from HIV-1-infected individuals display a proapoptotic profile characterized by decreased Bcl-2 levels and by caspase-3+ frequencies that are associated with levels of plasma viremia and T cell activation in an exploratory study. J. Virol. *85*, 397–409. https://doi.org/10.1128/JVI.01118-10.

20. Donaghy, H., Pozniak, A., Gazzard, B., Qazi, N., Gilmour, J., Gotch, F., and Patterson, S. (2001). Loss of blood CD11c(+) myeloid and CD11c(-) plasmacytoid dendritic cells in patients with HIV-1 infection correlates with HIV-1 RNA virus load. Blood *98*, 2574–2576. https://doi.org/10.1182/blood.v98.8.2574.

21. Huang, J., Al-Mozaini, M., Rogich, J., Carrington, M.F., Seiss, K., Pereyra, F., Lichterfeld, M., and Yu, X.G. (2012). Systemic inhibition of myeloid dendritic cells by circulating HLA class I molecules in HIV-1 infection. Retrovirology *9*, 11. https://doi.org/10.1186/1742-4690-9-11.

22. Dutertre, C.A., Amraoui, S., DeRosa, A., Jourdain, J.P., Vimeux, L., Goguet, M., Degrelle, S., Feuillet, V., Liovat, A.S., Müller-Trutwin, M., et al. (2012). Pivotal role of M-DC8(+) monocytes from viremic HIV-infected patients in TNFalpha overproduction in response to microbial products. Blood *120*, 2259–2268. https://doi.org/10.1182/blood-2012-03-418681.

23. Isnard, S., Hatton, E.X., Iannetta, M., Guillerme, J.B., and Hosmalin, A. (2021). Cell-Associated HIV Cross-Presentation by Plasmacytoid Dendritic Cells Is Potentiated by Noncognate CD8(+) T Cell Preactivation. J. Immunol. *207*, 15–22. https://doi.org/10.4049/jimmunol.2000392.

24. Beignon, A.S., McKenna, K., Skoberne, M., Manches, O., DaSilva, I., Kavanagh, D.G., Larsson, M., Gorelick, R.J., Lifson, J.D., and Bhardwaj, N. (2005). Endocytosis of HIV-1 activates plasmacytoid dendritic cells via Toll-like receptor-viral RNA interactions. J. Clin. Invest. *115*, 3265–3275. https://doi.org/10.1172/JCI26032.

25. Li, G., Cheng, M., Nunoya, J.I., Cheng, L., Guo, H., Yu, H., Liu, Y.J., Su, L., and Zhang, L. (2014). Plasmacytoid dendritic cells suppress HIV-1 replication but contribute to HIV-1 induced immunopathogenesis in humanized mice. PLoS Pathog. *10*, e1004291. https://doi.org/10.1371/journal.ppat.1004291.

26. Tomasello, E., Pollet, E., Vu Manh, T.P., Uzé, G., and Dalod, M. (2014). Harnessing Mechanistic Knowledge on Beneficial Versus Deleterious IFN-I Effects to Design Innovative Immunotherapies Targeting Cytokine Activity to Specific Cell Types. Front. Immunol. *5*, 526. https://doi.org/10.3389/fimmu.2014.00526.

27. Meier, A., Chang, J.J., Chan, E.S., Pollard, R.B., Sidhu, H.K., Kulkarni, S., Wen, T.F., Lindsay, R.J., Orellana, L., Mildvan, D., et al. (2009). Sex differences in the Toll-like receptor-mediated response of plasmacytoid dendritic cells to HIV-1. Nat. Med. *15*, 955–959. https://doi.org/10.1038/nm.2004.

28. Sandler, N.G., Bosinger, S.E., Estes, J.D., Zhu, R.T.R., Tharp, G.K., Boritz, E., Levin, D., Wijeyesinghe, S., Makamdop, K.N., del Prete, G.Q., et al. (2014). Type I interferon responses in rhesus macaques prevent SIV infection and slow disease progression. Nature *511*, 601–605. https://doi.org/10.1038/nature13554.

29. Silvin, A., Yu, C.I., Lahaye, X., Imperatore, F., Brault, J.B., Cardinaud, S., Becker, C., Kwan, W.H., Conrad, C., Maurin, M., et al. (2017). Constitutive resistance to viral infection in human CD141(+) dendritic cells. Sci. Immunol. *2*, eaai8071. https://doi.org/10.1126/sciimmunol.aai8071.

30. Cameron, P.U., Freudenthal, P.S., Barker, J.M., Gezelter, S., Inaba, K., and Steinman, R.M. (1992). Dendritic cells exposed to human immunodeficiency virus type-1 transmit a vigorous cytopathic infection to CD4+ T cells. Science *257*, 383–387. https://doi.org/10.1126/science.1352913.

31. Izquierdo-Useros, N., Lorizate, M., Contreras, F.X., Rodriguez-Plata, M.T., Glass, B., Erkizia, I., Prado, J.G., Casas, J., Fabriàs, G., Kräusslich, H.G., and Martinez-Picado, J. (2012). Sialyllactose in viral membrane gangliosides is a novel molecular recognition pattern for mature dendritic cell capture of HIV-1. PLoS Biol. *10*, e1001315. https://doi.org/10.1371/journal.pbio.1001315.

32. Izquierdo-Useros, N., Lorizate, M., McLaren, P.J., Telenti, A., Kräusslich, H.G., and Martinez-Picado, J. (2014). HIV-1 capture and transmission by dendritic cells: the role of viral glycolipids and the cellular receptor Siglec-1. PLoS Pathog. *10*, e1004146. https://doi.org/10.1371/journal.ppat.1004146.

33. Loré, K., Smed-Sörensen, A., Vasudevan, J., Mascola, J.R., and Koup, R.A. (2005). Myeloid and plasmacytoid dendritic cells transfer HIV-1 preferentially to antigen-specific CD4+ T cells. J. Exp. Med. *201*, 2023–2033. https://doi.org/10.1084/jem.20042413.

34. Ménager, M.M., and Littman, D.R. (2016). Actin Dynamics Regulates Dendritic Cell-Mediated Transfer of HIV-1 to T Cells. Cell *164*, 695–709. https://doi.org/10.1016/j.cell.2015.12.036.

35. Sandgren, K.J., Smed-Sörensen, A., Forsell, M.N., Soldemo, M., Adams, W.C., Liang, F., Perbeck, L., Koup, R.A., Wyatt, R.T., Karlsson Hedestam, G.B., and Loré, K. (2013). Human plasmacytoid dendritic cells efficiently capture HIV-1 envelope glycoproteins via CD4 for antigen presentation. J. Immunol. *191*, 60–69. https://doi.org/10.4049/jimmunol.1202489.

36. Wu, L., and KewalRamani, V.N. (2006). Dendritic-cell interactions with HIV: infection and viral dissemination. Nat. Rev. Immunol. *6*, 859–868. https://doi.org/10.1038/nri1960.

37. Brouiller, F., Nadalin, F., Bonté, P.E., Ait-Mohamed, O., Delaugerre, C., Lelièvre, J.D., Ginhoux, F., Ruffin, N., and Benaroch, P. (2023). Single-cell RNA-seq analysis reveals dual sensing of HIV-1 in blood Axl(+) dendritic cells. iScience *26*, 106019. https://doi.org/10.1016/j.isci.2023.106019.

38. Ruffin, N., Gea-Mallorquí, E., Brouiller, F., Jouve, M., Silvin, A., See, P., Dutertre, C.A., Ginhoux, F., and Benaroch, P. (2019). Constitutive Siglec-1 expression confers susceptibility to HIV-1 infection of human dendritic cell precursors. Proc. Natl. Acad. Sci. USA *116*, 21685–21693. https://doi.org/10.1073/pnas.1911007116.

39. Alaoui, L., Palomino, G., Zurawski, S., Zurawski, G., Coindre, S., Dereuddre-Bosquet, N., Lecuroux, C., Goujard, C., Vaslin, B., Bourgeois, C., et al. (2018). Early SIV and HIV infection promotes the LILRB2/MHC-I inhibitory axis in cDCs. Cell. Mol. Life Sci. *75*, 1871–1887. https://doi.org/10.1007/s00018-017-2712-9.

40. Barratt-Boyes, S.M., Brown, K.N., Melhem, N., Soloff, A.C., and Gleason, S.M. (2006). Understanding and exploiting dendritic cells in human immunodeficiency virus infection using the nonhuman primate model. Immunol. Res. *36*, 265–274. https://doi.org/10.1385/IR:36:1:265.

41. Kader, M., Smith, A.P., Guiducci, C., Wonderlich, E.R., Normolle, D., Watkins, S.C., Barrat, F.J., and Barratt-Boyes, S.M. (2013). Blocking TLR7- and TLR9-mediated IFN-alpha production by plasmacytoid dendritic cells does not diminish immune activation in early SIV infection. PLoS Pathog. *9*, e1003530. https://doi.org/10.1371/journal.ppat.1003530.

42. Malleret, B., Karlsson, I., Manéglier, B., Brochard, P., Delache, B., Andrieu, T., Muller-Trutwin, M., Beaumont, T., McCune, J.M., Banchereau, J., et al. (2008). Effect of SIVmac infection on plasmacytoid and CD1c+ myeloid dendritic cells in cynomolgus macaques. Immunology *124*, 223–233. https://doi.org/10.1111/j.1365-2567.2007.02758.x.

43. Malleret, B., Manéglier, B., Karlsson, I., Lebon, P., Nascimbeni, M., Perié, L., Brochard, P., Delache, B., Calvo, J., Andrieu, T., et al. (2008). Primary infection with simian immunodeficiency virus: plasmacytoid dendritic cell homing to lymph nodes, type I interferon, and immune suppression. Blood *112*, 4598–4608. https://doi.org/10.1182/blood-2008-06-162651.

44. Wonderlich, E.R., Kader, M., Wijewardana, V., and Barratt-Boyes, S.M. (2011). Dissecting the role of dendritic cells in simian immunodeficiency virus infection and AIDS. Immunol. Res. *50*, 228–234. https://doi.org/10.1007/s12026-011-8220-3.

45. Lee, M.Y.H., Upadhyay, A.A., Walum, H., Chan, C.N., Dawoud, R.A., Grech, C., Harper, J.L., Karunakaran, K.A., Nelson, S.A., Mahar, E.A., et al. (2021). Tissue-specific transcriptional profiling of plasmacytoid dendritic cells reveals a hyperactivated state in chronic SIV infection. PLoS Pathog. *17*, e1009674. https://doi.org/10.1371/journal.ppat.1009674.

46. Bjornson-Hooper, Z.B., Fragiadakis, G.K., Spitzer, M.H., Chen, H., Madhireddy, D., Hu, K., Lundsten, K., McIlwain, D.R., and Nolan, G.P. (2022). A Comprehensive Atlas of Immunological Differences Between Humans, Mice, and Non-Human Primates. Front. Immunol. *13*, 867015. https://doi.org/10.3389/fimmu.2022.867015.

47. Alcántara-Hernández, M., Leylek, R., Wagar, L.E., Engleman, E.G., Keler, T., Marinkovich, M.P., Davis, M.M., Nolan, G.P., and Idoyaga, J. (2017). High-Dimensional Phenotypic Mapping of Human Dendritic Cells Reveals Interindividual Variation and Tissue Specialization. Immunity *47*, 1037–1050.e6. https://doi.org/10.1016/j.immuni.2017.11.001.

48. Cabeza-Cabrerizo, M., van Blijswijk, J., Wienert, S., Heim, D., Jenkins, R.P., Chakravarty, P., Rogers, N., Frederico, B., Acton, S., Beerling, E., et al. (2019). Tissue clonality of dendritic cell subsets and emergency DCpoiesis revealed by multicolor fate mapping of DC progenitors. Sci. Immunol. *4*, eaaw1941. https://doi.org/10.1126/sciimmunol.aaw1941.

49. Leylek, R., Alcántara-Hernández, M., Lanzar, Z., Lüdtke, A., Perez, O.A., Reizis, B., and Idoyaga, J. (2019). Integrated Cross-Species Analysis Identifies a Conserved Transitional Dendritic Cell Population. Cell Rep. *29*, 3736–3750.e8. https://doi.org/10.1016/j.celrep.2019.11.042.

50. Schlitzer, A., Sivakamasundari, V., Chen, J., Sumatoh, H.R.B., Schreuder, J., Lum, J., Malleret, B., Zhang, S., Larbi, A., Zolezzi, F., et al. (2015). Identification of cDC1- and cDC2-committed DC progenitors reveals early lineage priming at the common DC progenitor stage in the bone marrow. Nat. Immunol. *16*, 718–728. https://doi.org/10.1038/ni.3200.

51. Bruel, T., Dupuy, S., Démoulins, T., Rogez-Kreuz, C., Dutrieux, J., Corneau, A., Cosma, A., Cheynier, R., Dereuddre-Bosquet, N., Le Grand, R., and Vaslin, B. (2014). Plasmacytoid dendritic cell dynamics tune interferon-alfa production in SIV-infected cynomolgus macaques. PLoS Pathog. *10*, e1003915. https://doi.org/10.1371/journal.ppat.1003915.

52. Wijewardana, V., Soloff, A.C., Liu, X., Brown, K.N., and Barratt-Boyes, S.M. (2010). Early myeloid dendritic cell dysregulation is predictive of disease progression in simian immunodeficiency virus infection. PLoS Pathog. *6*, e1001235. https://doi.org/10.1371/journal.ppat.1001235.

53. Wonderlich, E.R., Wu, W.C., Normolle, D.P., and Barratt-Boyes, S.M. (2015). Macrophages and Myeloid Dendritic Cells Lose T Cell-Stimulating Function in Simian Immunodeficiency Virus Infection Associated with Diminished IL-12 and IFN-alpha Production. J. Immunol. *195*, 3284–3292. https://doi.org/10.4049/jimmunol.1500683.

54. Autissier, P., Soulas, C., Burdo, T.H., and Williams, K.C. (2010). Immunophenotyping of lymphocyte, monocyte and dendritic cell subsets in normal rhesus macaques by 12-color flow cytometry: clarification on DC heterogeneity. J. Immunol. Methods *360*, 119–128. https://doi.org/10.1016/j.jim.2010.06.017.

55. Brown, K.N., and Barratt-Boyes, S.M. (2009). Surface phenotype and rapid quantification of blood dendritic cell subsets in the rhesus macaque. J. Med. Primatol. *38*, 272–278. https://doi.org/10.1111/j.1600-0684.2009.00353.x.

56. Dutertre, C.A., Jourdain, J.P., Rancez, M., Amraoui, S., Fossum, E., Bogen, B., Sanchez, C., Couëdel-Courteille, A., Richard, Y., Dalod, M., et al. (2014). TLR3-responsive, XCR1+, CD141(BDCA-3)+/CD8alpha+-equivalent dendritic cells uncovered in healthy and simian immunodeficiency virus-infected rhesus macaques. J. Immunol. *192*, 4697–4708. https://doi.org/10.4049/jimmunol.1302448.

57. Beshara, R., Sencio, V., Soulard, D., Barthélémy, A., Fontaine, J., Pinteau, T., Deruyter, L., Ismail, M.B., Paget, C., Sirard, J.C., et al. (2018). Alteration of Flt3-Ligand-dependent de novo generation of conventional dendritic cells during influenza infection contributes to respiratory bacterial superinfection. PLoS Pathog. *14*, e1007360. https://doi.org/10.1371/journal.ppat.1007360.

58. Cabeza-Cabrerizo, M., Minutti, C.M., da Costa, M.P., Cardoso, A., Jenkins, R.P., Kulikauskaite, J., Buck, M.D., Piot, C., Rogers, N., Crotta, S., et al. (2021). Recruitment of dendritic cell progenitors to foci of influenza A virus infection sustains immunity. Sci. Immunol. *6*, eabi9331. https://doi.org/10.1126/sciimmunol.abi9331.

59. Brown, K.N., Wijewardana, V., Liu, X., and Barratt-Boyes, S.M. (2009). Rapid influx and death of plasmacytoid dendritic cells in lymph nodes

mediate depletion in acute simian immunodeficiency virus infection. PLoS Pathog. *5*, e1000413. https://doi.org/10.1371/journal.ppat.1000413.

60. Laforge, M., Campillo-Gimenez, L., Monceaux, V., Cumont, M.C., Hurtrel, B., Corbeil, J., Zaunders, J., Elbim, C., and Estaquier, J. (2011). HIV/SIV infection primes monocytes and dendritic cells for apoptosis. PLoS Pathog. *7*, e1002087. https://doi.org/10.1371/journal.ppat.1002087.
61. Wijewardana, V., Bouwer, A.L., Brown, K.N., Liu, X., and Barratt-Boyes, S.M. (2014). Accumulation of functionally immature myeloid dendritic cells in lymph nodes of rhesus macaques with acute pathogenic simian immunodeficiency virus infection. Immunology *143*, 146–154. https://doi.org/10.1111/imm.12295.
62. Ferlazzo, G., Pack, M., Thomas, D., Paludan, C., Schmid, D., Strowig, T., Bougras, G., Muller, W.A., Moretta, L., and Münz, C. (2004). Distinct roles of IL-12 and IL-15 in human natural killer cell activation by dendritic cells from secondary lymphoid organs. Proc. Natl. Acad. Sci. USA *101*, 16606–16611. https://doi.org/10.1073/pnas.0407522101.
63. Kaplan, M.H., Sun, Y.L., Hoey, T., and Grusby, M.J. (1996). Impaired IL-12 responses and enhanced development of Th2 cells in Stat4-deficient mice. Nature *382*, 174–177. https://doi.org/10.1038/382174a0.
64. Louis, S., Dutertre, C.A., Vimeux, L., Fery, L., Henno, L., Diocou, S., Kahi, S., Deveau, C., Meyer, L., Goujard, C., and Hosmalin, A. (2010). IL-23 and IL-12p70 production by monocytes and dendritic cells in primary HIV-1 infection. J. Leukoc. Biol. *87*, 645–653. https://doi.org/10.1189/jlb.1009684.
65. Miller, E.A., Spadaccia, M.R., O'Brien, M.P., Rolnitzky, L., Sabado, R., Manches, O., Frleta, D., and Bhardwaj, N. (2012). Plasma factors during chronic HIV-1 infection impair IL-12 secretion by myeloid dendritic cells via a virus-independent pathway. J. Acquir. Immune Defic. Syndr. *61*, 535–544. https://doi.org/10.1097/QAI.0b013e31826afbce.
66. Bourdely, P., Anselmi, G., Vaivode, K., Ramos, R.N., Missolo-Koussou, Y., Hidalgo, S., Tosselo, J., Nuñez, N., Richer, W., Vincent-Salomon, A., et al. (2020). Transcriptional and Functional Analysis of CD1c(+) Human Dendritic Cells Identifies a CD163(+) Subset Priming CD8(+)CD103(+) T Cells. Immunity *53*, 335–352.e8. https://doi.org/10.1016/j.immuni.2020.06.002.
67. Collins, D.R., Gaiha, G.D., and Walker, B.D. (2020). CD8(+) T cells in HIV control, cure and prevention. Nat. Rev. Immunol. *20*, 471–482. https://doi.org/10.1038/s41577-020-0274-9.
68. Brenchley, J.M., and Douek, D.C. (2008). HIV infection and the gastrointestinal immune system. Mucosal Immunol. *1*, 23–30. https://doi.org/10.1038/mi.2007.1.
69. Rivera, C.A., Randrian, V., Richer, W., Gerber-Ferder, Y., Delgado, M.G., Chikina, A.S., Frede, A., Sorini, C., Maurin, M., Kammoun-Chaari, H., et al. (2022). Epithelial colonization by gut dendritic cells promotes their functional diversification. Immunity *55*, 129–144.e8. https://doi.org/10.1016/j.immuni.2021.11.008.
70. Karlsson, I., Malleret, B., Brochard, P., Delache, B., Calvo, J., Le Grand, R., and Vaslin, B. (2007). Dynamics of T-cell responses and memory T cells during primary simian immunodeficiency virus infection in cynomolgus macaques. J. Virol. *81*, 13456–13468. https://doi.org/10.1128/JVI.01619-07.

STAR★METHODS

KEY RESOURCES TABLE

REAGENT or RESOURCE	SOURCE	IDENTIFIER
Antibodies		
Anti-human SynCAM (TSLC1/CADM1)	Cliniscience	Cat# CM004-3; RRID:AB_592783
Anti-human AXL BV650 (clone 108724)	BD	Cat# 747860 ; RRID:AB_2872322
Anti-human AXL AF700 (clone FAB154N)	R&D System	Cat# FAB154N
Anti-human BDCA-2 PEVIO615 (clone AC144)	Miltenyi	Cat# 130113194; RRID:AB_2726019
Anti-human BDCA-2 APC (clone AC144)	Miltenyi	Cat# 130113190 ; RRID:AB_2726015
Anti-human CD11b BV785 (clone ICRF44)	Sony	Cat# 2106730
Anti-human CD11b BV711 (clone ICRF44)	Biolegend	Cat# 301344; RRID:AB_2563792
Anti-human CD11c BV650 (clone 3,9)	Biolegend	Cat# 301638; RRID:AB_2562231
Anti-human CD123 PerCP-cy5.5 (clone 7G3)	BD	Cat# 558714; RRID:AB_1645547
Anti-human CD14 V450 (clone M5E2)	BD	Cat# 558121; RRID:AB_397041
Anti-human CD14 V500 (clone M5E2)	BD	Cat# 561391; RRID:AB_10611856
Anti-human CD16 V450 (clone 3G8)	BD	Cat# 560474; RRID:AB_1645561
Anti-human CD141 BV711 (clone 1A4)	BD	Cat# 563155; RRID:AB_2738033
Anti-human CD141 PE (clone 1A4)	BD	Cat# 559781; RRID:AB_397322
Anti-human CD163 BB515 (clone REA812)	Miltenyi	Cat# 130-112-285; RRID:AB_2904769
Anti-human CD19 V450 (clone HIB19)	Sony	Cat# 2111160
Anti-human CD1c APCcy7 (clone L161)	Biolegend	Cat# 331520; RRID:AB_10644008
Anti-human CD1c PEdazzle (clone L161)	Biolegend	Cat# 331532; RRID:AB_2565293
Anti-human CD20 V450 (clone L27)	BD	Cat# 655872; RRID:AB_2870389
Anti-human CD3 V450 (clone SP34-2)	BD	Cat# 560351; RRID:AB_1645168
Anti-human CD33 PE (clone AC104,3E3)	Miltenyi	Cat# 130-113-349; RRID:AB_2726124
Anti-human CD34 pacific blue (clone 581)	Sony	Cat# 2317560
Anti-human CD40 APC (clone 5C3)	Biolegend	Cat# 334310; RRID:AB_2075792
Anti-human CD45 V500 (clone HI30)	BD	Cat# 560777; RRID:AB_1937324
Anti-NHP CD45 V500 (clone D058-1283)	BD	Cat# 561489; RRID:AB_10683313
Anti-human CD45RA BV785 (clone 5H9)	BD	Cat# 741010; RRID:AB_2740633
Anti-human CD5 PE (clone REA782)	BD	Cat# 130-110-990; RRID:AB_2658593
Anti-human CD56 V450 (clone B159)	BD	Cat# 560360; RRID:AB_1645578
Anti-human CD7 eFluor450 (clone 124-1D1)	Fisher Scientific	Cat# 15539626
Anti-human CD8 V450 (clone RPA-T8)	BD	Cat# 560347; RRID:AB_1645581
Anti-human CD80 PEcy7 (clone L307.4)	BD	Cat# 561135; RRID:AB_10561688
Anti-human CD83 FITC (clone HB15)	Biolegend	Cat# 305306; RRID:AB_314514
Anti-human CD86 BUV737 (clone 2331)	BD	Cat# 563412; RRID:AB_2916294
Anti-human CD88 PEcy7 (clone S5/1)	Miltenyi	Cat# 130-104-287; RRID:AB_2659435
Anti-human CD95 APC (clone DX2)	BD	Cat# 558814; RRID:AB_398659
Donkey anti-chicken FITC	Jackson immunoresearch	Cat# 703096155; RRID:AB_2340357
Donkey anti-chicken PE	Jackson immunoresearch	Cat# 703116155; RRID:AB_2340358
Anti-human HLADR AF700 (clone L243-G46-6)	Biolegend	Cat# 307626; RRID:AB_493771
Anti-human HLADR APC-cy7 (clone L243-G46-6)	Biolegend	Cat# 307618; RRID:AB_493587
Anti-human IFN-α PE (clone LT27:295)	Miltenyi	Cat# 130-092-601; RRID:AB_871560
Anti-human IL-12/IL-23 p40 BIOTIN (clone C8.6)	Biolegend	Cat# 508801; RRID:AB_315529
Anti-human Ki67 BV786 (clone B56)	BD	Cat# 563756; RRID:AB_2732007
Anti-human Siglec-1 PE-VIO770 (clone 7–239)	Miltenyi	Cat# 130-098-640; RRID:AB_2655549

(*Continued on next page*)

Continued

REAGENT or RESOURCE	SOURCE	IDENTIFIER
Anti-human Siglec-1 PE (clone 7-239)	Miltenyi	Cat# 130-098-654; RRID:AB_2655545
Anti-human Siglec-6 PE (clone FAB2859P)	R&D System	Cat# FAB2859P; RRID:AB_2714157
Anti-human TIGIT PerCP-eFluor™ 710 (clone MBSA43)	ebioscience	Cat# 46950042; RRID:AB_10853679
Anti-human TNF-α AF700 (clone MAB11)	Biolegend	Cat# 502928; RRID:AB_2561314
Streptavidin BV650	Biolegend	Cat# 405232
Biological samples		
Whole Blood from non-infected donors	Etablissement Français du Sang	N/A
Whole Blood from PLWH	ANRS C06 ANRS PRIMO cohort and ANRS C021 CODEX	N/A
Whole Blood from Cynomolgus macaques	IDMIT Facility	N/A
Tissues from Cynomolgus macaques	IDMIT Facility	N/A
Critical commercial assays		
Foxp3/Transcription Factor Staining Buffer Set	Invitrogen™ eBioscience™	Cat# 00-5523-00
PermWash 1X solution	Invitrogen™ eBioscience™	Cat# 00-8333-56
Permeabilization Buffer (10X)	Invitrogen™ eBioscience™	Cat# 12766048
Live/Dead Fixable Blue Dead	FISHER SCIENTIFIC SAS	Cat# 10114812
Software and algorithms		
FlowJo Software v10.0.8	BD Bioscience	https://www.flowjo.com/solutions/flowjo/downloads
GraphPad Prism 8	GraphPad Software, Inc.	https://www.graphpad.com/scientific-software/prism/
Other		
Ficoll	Eurobio	Cat# CMSMSL01-01
Fetal Bovine Serum	Sigma Aldrich	Cat# F7524
RPMI 1640 GlutaMAX	Gibco	Cat# 61870-010
Penicillin Streptomycin Neomycin	Gibco	Cat# 15640-055
Sodium pyruvate 1X	Thermo Fisher	Cat# 11360039
GentleMACS tubes	Miltenyi	Cat# 130-093-237
Macaque serum	IDMIT Facility	N/A
PBS	Gibco	Cat# 14190-094
Staining buffer	BD Pharmingen	Cat# 554657
R848/Resiquimod	Sigma	Cat# SML0196
LPS	Invivogen	Cat# TLRL-SMLPS
Poly(I:C) HMW	Invivogen	Cat# tlrl-pic
BFA	Sigma	Cat# B-7651
CellFix Solution	FISHER SCIENTIFIC SAS	Cat# 12756879

RESOURCE AVAILABILITY

Lead contact

Further information and requests for resources and reagents should be directed to the lead contact, Benoit Favier (benoit.favier@cea.fr).

Materials availability

This study did not generate new unique reagents. Requests for materials will require specific agreements and should be address to the lead contact, Benoit Favier.

Data and code availability

- All data reported in this paper will be shared by the lead contact upon request.

- This paper does not report original code.
- Any additional information required to reanalyze the data reported in this work paper is available from the lead contact upon request.

EXPERIMENTAL MODEL AND STUDY PARTICIPANT DETAILS

Macaca fascicularis were imported from Mauritius Island, and housed in Infectious Diseases Models and Innovative Therapies (IDMIT) laboratory belonging to the ''Commissariat à l'Energie Atomique et aux Energies Alternatives'' (CEA, Fontenay-aux-Roses, France. Animal studies was approved by the ethics committee ''Comité d'éthique en expérimentation animale'' No. 44, and by the ''Ministère de l'Education Nationale, de l'Enseignement Supérieur et de la Recherche'' (France) (reference 2015102713323361.02 (APAFIS▸2453)). All animal treatments and procedures were performed according to French national regulations and, by association, European regulations under the direct supervision of national veterinary inspectors (CEA accreditation No. D92-032-02) (European Directive 2010/63, recommendation No. 9), in compliance with the Standards for Human Care of the Office for Laboratory Animal Welfare (OLAW, USA; under OLAW Assurance No. A5826-01).

Macaque	Species	Sex	Age at the inclusion in the study
BA881J	Cynomolgus Macaque/Macaca fascicularis	Male	8
BA989J	Cynomolgus Macaque/Macaca fascicularis	Male	6
BC618D	Cynomolgus Macaque/Macaca fascicularis	Male	7
BC803C	Cynomolgus Macaque/Macaca fascicularis	Male	8
CB762B	Cynomolgus Macaque/Macaca fascicularis	Male	6
MF1308	Cynomolgus Macaque/Macaca fascicularis	Male	5
MF1309	Cynomolgus Macaque/Macaca fascicularis	Male	5
MF1412	Cynomolgus Macaque/Macaca fascicularis	Male	4
BA671L	Cynomolgus Macaque/Macaca fascicularis	Male	6
BB750G	Cynomolgus Macaque/Macaca fascicularis	Male	7
BA763N	Cynomolgus Macaque/Macaca fascicularis	Male	6
MF1405	Cynomolgus Macaque/Macaca fascicularis	Male	4

For PLWH, samples were processed from two different cohorts. The C06 ANRS PRIMO cohort was approved by the Paris-Cochin ethics committee. Blood samples were collected from PLWH at enrollment, before any treatment, and 1 year after effective combination ART. Primary infection phase was defined by negative or indeterminate HIV ELISA results, but with either p24 antigen$^+$, HIV-RNA$^+$ plasma, with an evolving western blot profile (no anti-Pol antibodies), or with a seronegative test performed less than 6 months prior to HIV$^+$ status. The CO21 ANRS CODEX Cohort was approved by the ethics committee of Ile de France VII. Elite Controller (EC) PLWH of this cohort were infection-positive for >5 years without ART. EC had the five last plasma HIV RNA test values below 400 copies/mL.[49] Blood samples of non-infected subjects were obtained from the ''*Etablissement Français du Sang*'' (EFS). All subjects gave written informed consent to participate in the study. Clinical parameters are summarized in Table S1.

METHOD DETAILS

SIV infections & sample collection

Cynomolgus macaques expressing the MHC-I H6 haplotype were excluded, as they are inclined to naturally control SIVmac251 viral infection. All procedures were performed under general anesthesia by intramuscular injection of 10 mg/mL Ketamine (Rhone-Merieux, Lyon, France). Animals were infected intravenously with a single 1000AID50 dose of SIVmac251 (n = 12) on day 0. From days 182–910, Group 1 received intravenous ART (emtricitabine and tenofovir disoproxil fumarate reverse transcriptase inhibitors (40 mg/kg, and 5.1 mg/kg, respectively), combined with dolutegravir integrase inhibitor (2.5 mg/kg)) daily.

Blood was collected in lithium heparin tubes (Vacutainer, BD, USA) and bone marrow was collected by aspiration from the iliac crest using an 18G syringe containing 10 mg/mL citrate dextrose. Lymph nodes were harvested from four different sites: right and left iliac and right and left axillary nodes. Spleens were collected at the time of euthanasia or when the clinical end points were reached.

SIV viral load quantification

Plasma from whole blood samples was obtained by centrifugation at 1500 x g for 10 min. SIV RNA was isolated from plasma using a High Pure viral RNA kit (Roche Diagnostics, Meylan), according to manufacturer specifications. Quantitative RT-PCR using primers towards the gag region of SIV genomic RNA was used to quantify plasma viral load, as previously described.[70]

Tissues processing

LN samples were divided in half with a scalpel before mechanical dissociation of single cells, by passing through a 70 μm nylon filter using gentle pressure applied with a sterile syringe plunger. The filter was washed with R10 media (RPMI 1640 GlutaMAX (Gibco) supplemented with 10% FBS (Sigma-Aldrich) + 1% Penicillin, Streptomycin, and Neomycin (Gibco)). Lymph node myeloid cells (LNMC) were recovered by centrifugation at 500 x g (4°C) for 10 min, and were resuspended in PBS 1X (Gibco). Peripheral blood mononuclear cells (PBMC) were isolated using a 1.077 density Ficoll cushion (Eurobio), centrifuged at 600 x g for 20 min, and resuspended in R10 media. Plasma was removed from bone marrow (BM) samples by centrifugation at 600 x g for 10 min, and then the cells were then resuspended in PBS before being overlaid onto a Ficoll gradient (as for blood, defined above). The layer of purified BM mononuclear cells (BMMC) were then recovered. Whole spleens were collected and transferred into GentleMACS tubes (Miltenyi), with RPMI medium (Gibco). GentleMACS dissociation was performed using manufacturer recommendations, and then samples were passed through a 100 μm nylon filter. Filtrate was diluted in PBS before Ficoll gradient purification, as described for blood samples above. All single cell suspension products were counted using a Vi-Cell XR automated hemocytometer (Beckman Coulter).

Antibody staining of cells & flow cytometry analysis

R10 media containing 10% macaque serum was used to saturate FcR binding sites to inhibit non-specific antibody staining at 4°C for 20 min. Antibody cocktails were prepared in staining buffer (BD Pharmingen) using previously calculated concentrations. Five million cells were labelled from each sample, first with anti-CADM1 + live/dead stain (Fisher Scientific), for 15 min at room temperature (RT) in the dark before washing with PBS 1X, then pelleting at 500 x g for 5 min. Then pellet was resuspended and incubation with remaining antibody cocktail was performed before being washed with PBS 1X and pelleting at 500 x g for 5 min. For Ki-67 intracellular staining, cells were permeabilized using the Foxp3/Transcription Factor Staining Buffer Set (Invitrogen) and stained in 1x PermWash (eBioscience) containing anti-Ki67 antibody (See key resources table) for 1 h at 4°C. Cells were then fixed with 1x Cell Fix (BD Biosciences), and acquired using a FORTESSA X20 flow cytometer (Becton Dickinson) and DIVA software. FlowJo v10.8.1. was used for analysis of all cytometry data. Antibody details are described in key resources table.

TLR agonist stimulation *ex vivo* & intracellular cytokine staining

Mononuclear cells from blood, LN or BM were stimulated for 3 h with 10 μg/mL R848/Resiquimod (Sigma), or 25 μg/mL PolyI:C (Invivogen), or 100 ng/mL LPS (Invivogen), diluted in RSG10 (RPMI medium +10% FCS + 1X Sodium pyruvate (Thermo Fisher) + 1% Glutamate). After 2 h of stimulation, Brefeldin A (10 μg/mL final concentration; Sigma) was added for one more hour. Cells were then washed and permeabilized using the Foxp3/Transcription Factor Staining Buffer Set (Invitrogen). Following the permeabilization step, FcR binding sites were saturated as described for antibody staining. For the final 20 min, a cocktail of anti-cytokine antibodies was added (See key resource reagents).

QUANTIFICATION AND STATISTICAL ANALYSIS

All statistical analyses were performed using Prism 9 (GraphPad Software). Statistical details of experiments are reported in the figure legends. Nonparametric Mann-Whitney U test, or a paired nonparametric Wilcoxon signed-rank test, were performed between unpaired or paired data, respectively. Friedman test was used to analyze longitudinal data. Comparisons of data between groups, or pooled sample analyses used a Kruskall Wallis test and post-hoc tests.